

1969

# General solution of an inelastic beam-column problem, September 1969 (70-13)

W. F. Chen

Follow this and additional works at: <http://preserve.lehigh.edu/engr-civil-environmental-fritz-lab-reports>

---

## Recommended Citation

Chen, W. F., "General solution of an inelastic beam-column problem, September 1969 (70-13)" (1969). *Fritz Laboratory Reports*. Paper 276.  
<http://preserve.lehigh.edu/engr-civil-environmental-fritz-lab-reports/276>

This Technical Report is brought to you for free and open access by the Civil and Environmental Engineering at Lehigh Preserve. It has been accepted for inclusion in Fritz Laboratory Reports by an authorized administrator of Lehigh Preserve. For more information, please contact [preserve@lehigh.edu](mailto:preserve@lehigh.edu).

LEHIGH UNIVERSITY INSTITUTE OF RESEARCH



Space Frames with Biaxial Loading in Columns

# GENERAL SOLUTION OF AN INELASTIC BEAM-COLUMN PROBLEM

by  
W. F. Chen

September 1969

Fritz Engineering Laboratory Report No. 331.5

Space Frames with Biaxial Loading in Columns

GENERAL SOLUTION OF AN INELASTIC  
BEAM-COLUMN PROBLEM

by

W. F. Chen

This work has been carried out as a part of an investigation sponsored jointly by the Welding Research Council and the Department of the Navy with funds furnished by the following:

American Iron and Steel Institute  
Naval Ships Systems Command  
Naval Facilities Engineering Command

Fritz Engineering Laboratory  
Department of Civil Engineering  
Lehigh University  
Bethlehem, Pennsylvania

September 1969

Fritz Engineering Laboratory Report No. 331.5

# GENERAL SOLUTION OF AN INELASTIC BEAM-COLUMN PROBLEM

by

W. F. Chen\*

## ABSTRACT

Analytical solutions that describe the elastic-plastic behavior of a beam-column loaded at the ends and the mid-span are presented. Much work has been done on the elastic solution, so the current effort is to extend this work to the inelastic range. Difficulties associated with the analysis are outlined, and the method of attack in overcoming these difficulties is described. The theoretical analysis of the six different cases which correspond to different stages of plastification within the beam-column is discussed. Interaction curves for combinations of axial force and lateral load that can be safely supported by the beam-column of rectangular and wide-flange cross sections are presented. The beam-column with an initial curvature is also discussed.

---

\* Assistant Professor, Fritz Engineering Laboratory, Department of Civil Engineering, Lehigh University, Bethlehem, Pennsylvania.

## TABLE OF CONTENTS

	<u>Page</u>
ABSTRACT	
1. INTRODUCTION	1
2. PREVIOUS WORK	3
3. STATEMENT OF THE BEAM-COLUMN PROBLEM	4
4. GENERALIZED MOMENT-CURVATURE-THRUST RELATIONSHIPS	6
5. DIFFERENTIAL EQUATIONS AND THEIR SOLUTIONS	15
6. DISCONTINUITY IN THE DERIVATIVE OF THE CURVATURE CURVE	18
7. SOLUTION OF THE ELASTIC BEAM-COLUMN - CASE 1	22
8. SOLUTION OF THE ELASTIC-PLASTIC BEAM-COLUMN YIELDED ON ONE-SIDE - CASE 2	25
9. SOLUTION OF THE ELASTIC-PLASTIC BEAM-COLUMN YIELDED ON TWO SIDES - CASE 4	31
10. NUMERICAL RESULTS	39
11. CONCLUSIONS	49
12. ACKNOWLEDGEMENTS	50
13. FIGURES	51
14. APPENDIX I - SOLUTION FOR CASE 3, CASE 5, AND CASE 6	70
15. APPENDIX II - SAMPLE CURVES	75
16. NOTATION	86
17. REFERENCES	88

## 1. INTRODUCTION

The elastic-plastic behavior of an eccentrically loaded beam-column under a concentrated load at the mid-span, as shown in Fig. 1, is an important technical problem with frequent engineering applications. The obvious example is a compression member in building frames; bridge trusses are another. It is also of great significance in the theory of structures because it is one of the simplest beam-column problems involving only simple loadings and boundary conditions. It is natural, therefore, to expect that this problem should possess a long history of study. Analytical solutions that describe the elastic behavior of beam-columns with various end conditions comprise the most highly developed aspect of beam-column research. Discussions of the solutions and theories are described admirably by Timoshenko and Gere [1]. Unfortunately, past attempts have not been successful in obtaining analytical solutions to beam-column problems composed of common structural sections when the beam-columns are stressed beyond the elastic limit. In part, this difficulty was caused by the inability to obtain a relatively simple moment-curvature-thrust relationship for commonly used structural sections. In addition, it is pointed out [2] that direct solutions to the differential equations of deflection are generally impossible to obtain because of the high nonlinearity of the basic equations.

A relatively easy alternative is to find a more appropriate variable than deflection for the elastic-plastic stability analysis, with a view to obtaining a relatively simple differential equation.

Curvature was demonstrated to be a more appropriate variable than deflection for the elastic-plastic analysis of eccentrically loaded columns in the paper cited [2]. This approach is adopted again in the present paper.

This paper is essentially a continuation of the paper referenced previously [2]. Here, the moment-curvature-thrust relationship derived in Reference 2 for a rectangular section is generalized to represent any complex shape of structural section to a high degree of approximation. The rectangular section is, of course, a special case of the generalized moment-curvature-thrust relationship. In addition, the generalized relationship also includes the idealized wide-flange and box sections of Hauck and Lee [3] (they assume the flange elements are very thin) as a special case with even better accuracy, so that it may be considered a generalization of their formulation.

## 2. PREVIOUS WORK

The elastic-plastic behavior of laterally loaded beam-columns has not been studied thoroughly, but a number of numerical solutions have been obtained. Wright developed an approximate formula for the case of a beam-column loaded by a concentrated load at the midspan (Fig. 1 set  $e = 0$ ) [4]. The same case was also studied by Ketter and interaction curves for predicting the strength of wide-flange beam-columns were developed [5]. Horne and Merchant [6] recently proposed an empirical method for estimating the strength of a beam-column. However, the validity of their method has not been verified by either numerical solutions or laboratory tests. More recently, Lu and Kamalvand [7], following the related work on eccentrically loaded columns of von Karman [8], Chwalla [9], and Ojalvo [10], extended the numerical integration procedure further to include the effect of the additional lateral load. The moment-curvature-thrust relationship used in their computations was represented in graphical form and programmed on a computer. Interaction curves for the ultimate lateral load carrying capacity of a variety of beam-columns were presented (for the case,  $e = 0$ ).



### 3. STATEMENT OF THE BEAM-COLUMN PROBLEM

The beam-column problem under consideration is shown in Fig. 1. Because of symmetry, only one half of the beam-column need be considered. It is therefore convenient to take the origin of the x-y axes at the left support of the beam-column, the x axis being directed along the member and the y axis being perpendicular to the x axis, positive downwards.

It is assumed that lateral-torsional buckling of the beam-column is effectively prevented so that failure is always caused by excessive bending in the plane of the applied loads. The axial force  $P$  at the ends of the beam-column is assumed to be applied first and maintained at a constant value as the lateral load  $Q$  increases or decreases. It is further assumed that for a given axial force, the curvature and the bending moment have one to one correspondence, and the actual history of loading does not affect the resulting moment-curvature-thrust relationship. This means that plastic straining is being assumed to be reversible. The second assumption on loading condition may be unnecessarily restrictive, but it does agree with the requirement that unloading of material stressed into the plastic range does not take place for an initially stress-free perfectly plastic beam-column. Furthermore, it will be seen later herein that such a loading condition can reduce greatly the work on the numerical evaluation of the solution for this problem. Other loading paths are, of course, permissible provided that the degree of unloading is small. For

example, a previous investigation [11] has indicated that the loads (axial force and lateral load) that are increased proportionately from zero do produce unloading but the effect appears to be small. The predicted collapse loads were found to be conservative. In the present analysis, irreversibility of plastic deformation in the beam-column is not attempted because it makes the solution highly complicated.

#### 4. GENERALIZED MOMENT-CURVATURE-THRUST RELATIONSHIPS

It is necessary to introduce non-dimensional quantities so that the moment-curvature-thrust relationship and hence the basic differential equations may be written in a form more appropriate for computation.

The initial yield quantities for moment,  $M$ ; axial force,  $P$ ; and curvature,  $\Phi$  of a section are defined by

$$M_y = \sigma_y S, \quad P_y = \sigma_y A, \quad \Phi_y = \frac{2 \epsilon_y}{h} \quad (1)$$

where  $\sigma_y$  is the yield stress in tension or compression and  $\epsilon_y$  is the corresponding strain. Other quantities used are: area,  $A$ ; elastic section modulus,  $S$ ; and height,  $h$ . One further defines the non-dimensional variables by

$$m = \frac{M}{M_y}, \quad p = \frac{P}{P_y}, \quad \varphi = \frac{\Phi}{\Phi_y} \quad (2)$$

A general  $m$ - $\varphi$ - $p$  curve of a common structural section with or without residual stress usually has the shape shown diagrammatically in Fig. 2. The curve may be divided into three regions: elastic, primary plastic, and secondary plastic. They are separated by the points  $(m_1, \varphi_1)$  and  $(m_2, \varphi_2)$  as shown in the figure. The general characteristic of such a curve is that the rate of curvature-hardening falls steadily, and the curve bends over more and more.

For a perfectly plastic material, the moment will asymptotically approach the value  $m_{pc}$  as  $\varphi$  tends to infinity but will not attain it for any finite curvature. In most metals, however, it is certainly realistic to assume that the limit value,  $m_{pc}$ , can actually be attained and even exceeded at a finite curvature because of strain hardening.

For a rectangular section of perfectly plastic material, the  $m$ - $\varphi$ - $p$  relationships for each region can be readily derived [2].

In the elastic range,

$$m = \varphi \quad (3)$$

valid for

$$0 \leq \varphi \leq 1-p \quad (4)$$

In the primary plastic range,

$$m = 3(1-p) - \frac{2(1-p)^{3/2}}{\varphi^{1/2}} \quad (5)$$

valid for

$$1-p \leq \varphi \leq \frac{1}{1-p} \quad (6)$$

In the secondary plastic range,

$$m = \frac{3}{2} (1-p^2) - \frac{1}{2 \varphi^2} \quad (7)$$

valid for

$$\frac{1}{1-p} \leq \varphi \quad (8)$$

More generally, when the  $m$ - $\varphi$ - $p$  curve is the type shown in Fig. 2, it appears reasonable to assume that the curve could be fitted by the following three equations. These equations are the direct generalization of the expressions derived previously for the rectangular section.

In the elastic region,

$$m = a \varphi \quad (9)$$

valid for

$$0 \leq \varphi \leq \varphi_1 \quad (10)$$

In the primary plastic region,

$$m = b - \frac{c}{\varphi^{1/2}} \quad (11)$$

valid for

$$\varphi_1 \leq \varphi \leq \varphi_2 \quad (12)$$

In the secondary plastic region,

$$m = m_{pc} - \frac{f}{\varphi^2} \quad (13)$$

valid for

$$\varphi_2 \leq \varphi \quad (14)$$

where  $a$ ,  $b$ ,  $c$ ,  $f$  are arbitrary constants. These constants can be evaluated easily by solving simultaneous equations which will arise if the particular values  $\varphi_1$ ,  $\varphi_2$ , and  $\varphi_\infty$  are inserted and the moments equated to the appropriate moments  $m_1$ ,  $m_2$ , and  $m_{pc}$ . As an example, this has been done for idealized wide-flange and box sections with very thin flange elements [3]. If  $R$  denotes the ratio of the sum of the flange areas to the sum of the web areas, for

$$p \geq \frac{1}{1+R} \quad (15)$$

these constants are

$$a = 1 \quad (16)$$

$$b = \frac{3(1+R)}{1+3R} (1-p) \quad (17)$$

$$c = \frac{2}{1+3R} (1-p)^{3/2} \quad (18)$$

valid for

$$\varphi_1 = 1-p \quad (19)$$

and

$$\varphi_2 = \infty \quad (20)$$

Here, as has been seen, secondary plastic  $m$ - $\varphi$ - $p$  relationships are absent, while the primary plastic  $m$ - $\varphi$ - $p$  relationships are extended from the elastic limit,  $\varphi_1 = 1-p$ , to infinity.

For

$$p \leq \frac{1}{1+R} \quad (21)$$

these constants are

$$a = 1 \quad (22)$$

$$b = 1-p + \frac{2p [ 1 + 2R - (1+R)^2 p ]}{(1 + 3R) \left\{ 1 - (1-p)^{1/2} [ 1 - (1+R) p ]^{1/2} \right\}} \quad (23)$$

$$c = \frac{2p (1-p)^{1/2} [ 1 + 2R - (1+R)^2 p ]}{(1 + 3R) \left\{ 1 - (1-p)^{1/2} [ 1 - (1+R) p ]^{1/2} \right\}} \quad (24)$$

$$f = \frac{1}{2 (1 + 3R)} \quad (25)$$

$$m_{pc} = \frac{3}{2} \frac{1 + 2R - (1+R)^2 p^2}{1 + 3R} \quad (26)$$

valid for

$$\varphi_1 = 1-p \quad (27)$$

and

$$\varphi_2 = \frac{1}{1 - (1+R) p} \quad (28)$$

Evidently the area ratio,  $R$ , assumes the value of zero for a rectangular cross section. The choice of  $R$  to fit the  $m$ - $\varphi$ - $p$  curves of commonly used thin-walled structural sections is not as obvious as it would seem to be. The details of the method and expression



are given by Hauck and Lee [3]. It was found that for a group of 50 commonly rolled wide-flange column sections, the range of  $R$  varied from 2.9 to 3.6 with the average value being approximately 3.27. The value 3.27 happens to be exact for the 8 W 31 section which has frequently been used in many investigations [5,7,10].

The  $m-\phi-p$  relationships for idealized thin-walled structural sections were derived in the paper cited [3]. The results are identical with the present expressions for the elastic range as well as for the secondary plastic range but different for the primary plastic range. Comparison of the curves obtained from the present expressions ( $R = 3.27$ ) with similar curves obtained for the actual shape of the section (8 W 31) [12] indicates that the tendency is to underestimate appreciably the actual moment where the curvature is in the primary plastic range, particularly in the region of initial yielding. This is a result of the fact that the power law between moment and curvature does not pick up sufficiently rapidly.

A relatively easy way to improve this deviation is to find a proper value for the constant,  $R$ . This proves very successful for the case of wide-flange sections without residual stress. For example, if the value of  $R$  is assumed to be 1.4 instead of 3.27, the actual  $m-\phi-p$  curves for the 8 W 31 section can be represented closely by the expressions described here. Figure 3 shows the plot of  $m$  versus  $\phi$  for several values of  $p$ . Comparison of these

curves with those obtained for the actual shape [12] indicates that the actual curves are generally too large by approximately 4 percent.

Although the stability analysis is concerned with the overall change of geometry of a member, the local plastic curvature is not too large compared with the elastic curvature. The theoretical results obtained in this paper indicate that when the curvature is a few times those at initial yield value, the applied load has reached already the value within a few percent of the load which produces collapse of the beam-column. Then the  $m-\phi-p$  curve for curvature up to a few times those at initial yield value is of primary interest. Therefore, a good curve fitting in the initial yielded region may be considered adequate for the study of stability problems.

Figure 4 shows the comparison of these curves for the value of  $R = 1$  instead of 1.4. Comparison of these curves for curvature up to the value of 2.5 indicates that the generalized expressions tend to underestimate the actual moment slightly where  $\phi$  is small and to overestimate the actual moment where  $\phi$  is large for the regions beyond initial yielding. For  $\phi$  less than 2.5, the maximum difference between the actual curves and the approximate curves is about 5 percent. In connection with a complete solution of the type to be described in this paper, the error will be much smaller because the approximate curve may be thought of as averaging its effect over the field of plastic deformation.

The present curves (Fig. 3) are seen to provide a better approximation than the results given by Hauck and Lee [3] for the overall range of curvature. For the particular 8 W 31 section cited, their results are generally too large by approximately 10 percent. However, it must be noted that the present approach of adjusting the value of  $R$  equal to 1 (Fig. 4) in order to give the best fit over the initial yielded curvature-range fails, of course, for very large curvature, since this would involve considerable error.

The  $m$ - $\phi$ - $p$  relationships for an arbitrary shape of structural section including the influence of residual stress can also be fitted by the generalized  $m$ - $\phi$ - $p$  relationships proposed here. Of course, equations 15 to 28 in their present forms do not apply to wide-flange sections with residual stress. Equations applicable to such sections will be developed in a later paper.

## 5. DIFFERENTIAL EQUATIONS AND THEIR SOLUTIONS

The equation of equilibrium for bending of the beam-column shown in Fig. 1 is, of course, independent of the mechanical behavior of the member. In the usual notation [1],

$$\frac{d^2 m}{dx^2} + k^2 \varphi = 0 \quad (29)$$

where  $k$  is given by:

$$k^2 = \frac{P \phi_y}{M_y} = \frac{P}{EI} \quad (30)$$

The quantity  $EI$  represents the flexural rigidity of the beam-column in the plane of bending. Combining the statical Equation (29) with the generalized  $m$ - $\varphi$ - $p$  relationships (9), (11), and (13), one can express the differential equations of the axis of the beam-column in the following forms:

### Elastic Zone

$$\frac{d^2 \varphi}{dx^2} + \frac{k^2}{a} \varphi = 0 \quad (31)$$

### Primary Plastic Zone

$$\varphi \frac{d^2 \varphi}{dx^2} - \frac{3}{2} \left( \frac{d\varphi}{dx} \right)^2 + \frac{2k^2}{c} \varphi^{7/2} = 0 \quad (32)$$

### Secondary Plastic Zone

$$\varphi \frac{d^2 \varphi}{dx^2} - 3 \left( \frac{d\varphi}{dx} \right)^2 + \frac{k^2}{2f} \varphi^5 = 0 \quad (33)$$

Equations (31), (32), and (33) are the basic differential equations for bending of beam-columns. If the constants  $a$ ,  $c$ , and  $f$  equal 1,  $2(1-p)^{3/2}$  and  $1/2$  respectively, these equations reduce to the equations developed previously for bending of a rectangular section [2].

Equations (32) and (33) are "exact" differential equations with  $\varphi^{-4}$  and  $\varphi^{-7}$  as the integral factors respectively.

Six integration constants are to be expected in a general solution of Equations (31), (32), and (33).

Proceeding with the solution, Equations (32) and (33) may be integrated once to give

### Primary Plastic Zone

$$\frac{d\varphi}{dx} = \frac{2\sqrt{2}k}{\sqrt{c}} (D - \varphi^{1/2})^{1/2} \varphi^{3/2} \quad (34)$$

### Secondary Plastic Range

$$\frac{d\varphi}{dx} = \frac{k}{\sqrt{f}} (1 + G\varphi)^{1/2} \varphi^{5/2} \quad (35)$$

In order to solve for the curvature, one has to integrate Equations (34) and (35) for the solution. It is difficult to express  $\varphi$

explicitly in terms of  $x$ . Alternatively, it is more convenient to express the curvature implicitly in the form  $x = x(\varphi)$ . The general solutions of the Equations (31), (34), and (35) are

#### Elastic Zone

$$\varphi = A_1 \cos \frac{kx}{\sqrt{a}} + B \sin \frac{kx}{\sqrt{a}} \quad (36)$$

#### Primary Plastic Zone

$$x - x_p = - \left( \frac{\sqrt{c}}{\sqrt{2k}} \right) \frac{1}{D} \left[ \frac{(D - \varphi^{1/2})^{1/2}}{\varphi^{1/2}} + \frac{1}{D^{1/2}} \tanh^{-1} \frac{(D - \varphi^{1/2})^{1/2}}{D^{1/2}} \right] \quad (37)$$

#### Secondary Plastic Zone

$$x - x_s = \frac{2}{3} \frac{\sqrt{f}}{k} \left( G + \frac{1}{\varphi} \right)^{1/2} \left( 2G - \frac{1}{\varphi} \right) \quad (38)$$

Thus, if the constants of integration  $A_1$ ,  $B$ ,  $D$ ,  $G$ ,  $x_p$ , and  $x_s$  in Equations (36), (37), and (38) are known from the boundary conditions of the beam-column and the continuity conditions of the curvature curves (or jump conditions discussed later in Section 6),  $x$  becomes a known function of  $\varphi$ . In general, there are six different distributions of stress zone possible as shown in Fig. 1. Hence, the constants corresponding to each case have to be considered separately. They will be discussed in some detail when the solution for each case is presented.

## 6. DISCONTINUITY IN THE DERIVATIVE OF THE CURVATURE CURVE

The analysis of the differential equations, developed generally in Section 5 (specialized later in Sections 7, 8, and 9 to the various individual cases) implicitly assumes that the curvature curve is a continuous differentiable function of  $x$ . However, consideration of the generalized  $m$ - $\varphi$ - $p$  relationship (Fig. 2) shows that too much should not be expected in the way of differentiability on the curvature curve. At the point  $\varphi = \varphi_1$  or  $\varphi = \varphi_2$ , two  $dm/d\varphi$  values are associated with the curvature. Any such discontinuity in the  $m$ - $\varphi$ - $p$  relationship will show up where it is applicable in the study of the solutions of the differential equations in general. In addition, discontinuity in the derivative of the curvature curve can also arise in the case when a concentrated load is present. In such a case, there is a discontinuity in the derivative of the curvature curve at the section where the concentrated load is applied. In all these circumstances, the "jump condition" (or discontinuity condition) instead of the continuity condition for the derivative of the curvature curve must be used locally for the determination of the integration constants. The purpose of the present discussion is to show how the permissible "jump conditions" are determined.

A beam-column, a moment diagram, and a curvature curve are sketched in Fig. 5. The jump in  $d\varphi/dx$  will occur either across the boundaries  $\rho_1$ ,  $\rho_2$ , or under the concentrated load  $Q$ . There will be two values of  $d\varphi/dx$  depending upon whether  $x$  is allowed to approach the jump from the right side or from the left side. In such cases,

it is convenient to adopt the following notation. If  $x \rightarrow \rho_1$ , say, from left (that is,  $x$  is always less than  $\rho_1$ ), one writes the left-hand limit of  $d\phi/dx$ , as

$$\left. \frac{d\phi}{dx} \right|_{x \rightarrow \rho_1^-} \quad \text{or} \quad \left. \frac{d\phi}{dx} \right|_{\rho_1^-} \quad (39)$$

and the fact that the value of  $d\phi/dx$  as  $x \rightarrow \rho_1$  from the right (so that  $x$  is always greater than  $\rho_1$ ) is denoted by

$$\left. \frac{d\phi}{dx} \right|_{x \rightarrow \rho_1^+} \quad \text{or} \quad \left. \frac{d\phi}{dx} \right|_{\rho_1^+} \quad (40)$$

also

$$\left. \frac{dm}{d\phi} \right|_{\phi \rightarrow \phi_1^-} \quad \text{or} \quad \left. \frac{dm}{d\phi} \right|_{\phi_1^-} \quad (41)$$

and

$$\left. \frac{dm}{d\phi} \right|_{\phi \rightarrow \phi_1^+} \quad \text{or} \quad \left. \frac{dm}{d\phi} \right|_{\phi_1^+} \quad (42)$$

will stand for the left-hand and right-hand limits of  $dm/d\phi$ .

#### Jumps in $d\phi/dx$ due to jumps in $m$ - $\phi$ - $p$ curve

(i) jump condition at the elastic-primary plastic boundary,

$$\underline{x = \rho_1}$$



Since the value  $dm/dx$  at  $x = \rho_1$  is continuous (see the sketched moment diagram in Fig. 4), it follows that

$$\left[ \frac{dm}{d\varphi} \right]_{\varphi_1} - \left[ \frac{d\varphi}{dx} \right]_{\rho_1} = \left[ \frac{dm}{d\varphi} \right]_{\varphi_1} + \left[ \frac{d\varphi}{dx} \right]_{\rho_1} + \quad (43)$$

or, using the  $m$ - $\varphi$ - $p$  relations (9) and (11), Equation (43) reduces to

$$\frac{2a}{c} \varphi_1^{3/2} \left[ \frac{d\varphi}{dx} \right]_{\rho_1} = \left[ \frac{d\varphi}{dx} \right]_{\rho_1} + \quad (44)$$

(ii) jump condition at the primary-secondary plastic boundary,

$$\underline{x = \rho_2}$$

Similarly, if  $\varphi_1$  and  $\rho_1$  in Equation (43) are substituted by  $\varphi_2$  and  $\rho_2$ , one obtains

$$\frac{c}{4f} \varphi_2^{3/2} \left[ \frac{d\varphi}{dx} \right]_{\rho_2} = \left[ \frac{d\varphi}{dx} \right]_{\rho_2} + \quad (45)$$

(iii) jump condition at elastic-secondary plastic boundary,

$$\underline{x = \rho_1 = \rho_2}$$

For the special case,  $p = 0$  (beam problem),  $\varphi_1 = \varphi_2$ , one obtains

$$\frac{a}{2f} \varphi_2^3 \left[ \frac{d\varphi}{dx} \right]_{\rho_2} = \left[ \frac{d\varphi}{dx} \right]_{\rho_2} + \quad (46)$$

Jumps in  $d\varphi/dx$  due to concentrated load

Since

$$\frac{d\varphi}{dx} = \frac{\frac{dm}{dx}}{\frac{dm}{d\varphi}} \quad (47)$$

It follows that the jump conditions under the concentrated load  $Q$  which is applied at the mid-section of the beam-column are (Fig. 5)

(i) elastic regime

$$\left. \frac{d\varphi}{dx} \right|_{x=\frac{l}{2}} = \frac{\frac{Q}{2M_y}}{a} = \frac{Q}{2aM_y} \quad (48)$$

(ii) primary plastic regime

$$\left. \frac{d\varphi}{dx} \right|_{x=\frac{l}{2}} = \frac{\frac{Q}{2M_y}}{\frac{c}{2\varphi_m^{3/2}}} = \frac{Q}{cM_y} \varphi_m^{3/2} \quad (49)$$

(iii) secondary plastic regime

$$\left. \frac{d\varphi}{dx} \right|_{x=\frac{l}{2}} = \frac{\frac{Q}{2M_y}}{\frac{2f}{\varphi_m^3}} = \frac{Q}{4fM_y} \varphi_m^3 \quad (50)$$

where  $\varphi_m$  denotes the curvature at the central cross section of the beam-column.

## 7. SOLUTION OF THE ELASTIC BEAM-COLUMN - CASE 1

In Fig. 1, Case 1, Case 2, and Case 4 are found to be of major importance in the practical application of beam-column solutions. For this reason, these three cases will be considered in detail in what follows, and the solutions for the other cases will be given in Appendix I.

The general solution of the elastic beam-column [Fig. 1 (a)] is given by Equation (36). Since the beam-column and the loading are symmetrical about the mid-section of the beam-column, it is necessary to consider only the portion to the left of the load.

The constants of integration  $A_1$  and  $B$  are determined from the conditions at the end of the beam-column and at the point of application of the load  $Q$ . Since the curvature at the end of the beam-column is  $\varphi_0 = m_0/a$  and the derivative of the curvature at the point of application of the load  $Q$  must satisfy the "jump condition" as given by Equation (48), one concludes that

$$A_1 = \frac{m_0}{a} \quad (51)$$

$$B = \frac{Q}{2\sqrt{a} kM_y} \sec \frac{k\ell}{2\sqrt{a}} + \frac{m_0}{a} \tan \frac{k\ell}{2\sqrt{a}} \quad (52)$$

where

$$m_o = \frac{1}{2} P \left(\frac{e}{r}\right) \left(\frac{h}{r}\right) \quad (53)$$

in which  $r$  is the radius of gyration of the section about the axis of bending and  $e$  is the eccentricity of the axial force  $P$ .

Substituting into Equation (36) the values of constants from Equations (51) and (52), one obtains the equation for the curvature curve

$$\varphi = \left[ \frac{m_o}{a} \cos \frac{k(\ell-2x)}{2\sqrt{a}} + \frac{2}{\sqrt{a}} \left(\frac{\alpha q}{k\ell}\right) \sin \frac{kx}{\sqrt{a}} \right] \sec \frac{k\ell}{2\sqrt{a}} \quad (54)$$

valid for

$$0 \leq x \leq \frac{\ell}{2}$$

in which  $q$  is the nondimensional lateral load and is given by

$$q = \frac{Q}{Q_p} = \frac{Q\ell}{4\alpha M_y} \quad (55)$$

where  $Q_p$  is the plastic limit load of the beam-column according to simple plastic theory and  $\alpha$  is the shape factor of the section about the axis of bending.

The maximum curvature occurs at the center, which is

$$\varphi_m = \varphi_{x=\ell/2} = \frac{m_o}{a} \sec \frac{k\ell}{2\sqrt{a}} + \frac{2}{\sqrt{a}} \left(\frac{\alpha q}{k\ell}\right) \tan \frac{k\ell}{2\sqrt{a}} \quad (56)$$

valid for

$$0 \leq \varphi_m \leq \varphi_1$$

Equation (54) shows that for a given longitudinal force the curvatures of an elastic beam-column are proportional to the lateral load  $q$ .

# 8. SOLUTION OF THE ELASTIC-PLASTIC BEAM-COLUMN YIELDED ON ONE-SIDE - CASE 2

Referring to Fig. 1(b) (Case 2), the primary plastic zone begins at a distance,  $\rho_1$ , from the ends. The curvature at the center of the beam-column is denoted by  $\varphi_m$ .

The elastic end portions of the beam-column will be investigated first. The general solution of this portion is given by Equation (36). The constants of integration  $A_1$  and B are now determined from the conditions at the end and at the elastic-primary boundary. Since the curvature at the end of the beam-column is  $\varphi_0 = m_0/a$  and, at the elastic-primary plastic boundary ( $x = \rho_1$ ) is  $\varphi_1$ , it follows that the equation for the curvature curve in the elastic zone is

$$\varphi = \left[ \frac{m_0}{a} \sin \frac{k(\rho_1 - x)}{\sqrt{a}} + \varphi_1 \sin \frac{kx}{\sqrt{a}} \right] \csc \frac{k\rho_1}{\sqrt{a}} \quad (57)$$

valid for

$$0 \leq x \leq \rho_1$$

The unknown distance  $\rho_1$  will be determined from the solution for the primary plastic zone.

The derivative of the curvature curve for the primary plastic zone is given by Equation (34). The constant D and the

unknown quantity,  $\varphi_m$ , can be determined from the "jump conditions" at the central cross section and at the section  $x = \rho_1$ . Since the derivative of the curvature curve at these two sections must satisfy the "jump conditions", as given by Equations (49) and (44), respectively, it can be concluded that

$$D = \varphi_1^{1/2} \eta \quad (58)$$

$$\varphi_m = \left[ \varphi_1^{1/2} \eta - \frac{2}{c} \left( \frac{\alpha q}{k\ell} \right)^2 \right]^2 \quad (59)$$

valid for

$$\varphi_1 \leq \varphi_m \leq \varphi_2$$

in which  $\eta$  is defined as

$$\eta = 1 + \frac{a}{2c} \varphi_1^{3/2} \left[ \cot \frac{k\rho_1}{\sqrt{a}} - \left( \frac{m_0}{a\varphi_1} \right) \csc \frac{k\rho_1}{\sqrt{a}} \right]^2 \quad (60)$$

The general solution of the curvature curve for the primary plastic zone is given by Equation (37). The constant  $x_p$  and the value  $\rho_1$  are found from the conditions that  $\varphi$  in Equation (37) must be equal to  $\varphi_m$  and  $\varphi_1$  for  $x = \ell/2$  and  $x = \rho_1$ , respectively. Using Equations (58) and (59), one obtains

$$\frac{x_p}{l} = \frac{1}{2} + \frac{\sqrt{c}}{\sqrt{2}} \frac{1}{\varphi_1^{3/4} \eta^{3/2}} \frac{1}{kl} \left\{ \frac{\sqrt{2} \sqrt{c} \varphi_1^{1/4} \eta^{1/2} (\frac{\alpha q}{kl})}{c \varphi_1^{1/2} \eta - 2 (\frac{\alpha q}{kl})^2} + \tanh^{-1} \left[ \frac{\sqrt{2}}{\sqrt{c}} \frac{1}{\varphi_1^{1/4} \eta^{1/2}} (\frac{\alpha q}{kl}) \right] \right\} \quad (61)$$

and

$$\frac{\rho_1}{l} = \frac{x_p}{l} - \frac{\sqrt{c}}{\sqrt{2}} \frac{1}{\varphi_1^{3/4} \eta^{3/2}} \frac{1}{kl} \left[ \eta^{1/2} (\eta-1)^{1/2} + \tanh^{-1} \left( 1 - \frac{1}{\eta} \right)^{1/2} \right] \quad (62)$$

For a given beam-column and for the known values of the constants which define the generalized  $m$ - $\varphi$ - $p$  relationship, Equation (62) represents the desired condition for the determination of the elastic-primary plastic boundary,  $\rho_1$ , which can be obtained by trial and error.

Values of  $\rho_1$  found from this equation lie between the limits  $l/2$  and  $\rho_1^l$  (as yet undefined,  $\rho_1^l \geq 0$ ). The value  $l/2$  corresponds to  $\varphi_m = \varphi_1$ , which means that the value of the load  $q$  (loaded from Case 1 to Case 2) is that value for which the elastic limit is reached at the central cross section. The load  $q$  is obtained by substituting  $\varphi_m = \varphi_1$  in Equation (56) or Equation (59), which gives

$$q_{\varphi_m = \varphi_1} = \frac{\sqrt{c}}{\sqrt{2}} \varphi_1^{1/4} \frac{kl}{\alpha} \left( \eta_{\rho_1 = l/2} - 1 \right)^{1/2} \quad (63)$$



When the central cross section curvature, as given by Equation (59), reaches  $\varphi_2$ , the value of  $q$  is

$$q_{\varphi_m = \varphi_2} = \frac{\sqrt{c}}{\sqrt{2}} \varphi_1^{1/4} \frac{k\ell}{\alpha} \left[ \eta - \frac{\varphi_2^{1/2}}{\varphi_1^{1/2}} \right]^{1/2} \quad (64)$$

and the corresponding lower limit value,  $\rho_1^l$ , of  $\rho_1$  can be found from Equation (62) by trial and error.

Let us assume that the end loadings ( $p$  and  $m_0$ ) are small enough to keep the whole beam-column in the elastic range. If the lateral load  $q$  is now gradually increased to its maximum and then drops off steadily beyond the maximum point, the curvature at the central cross section of the beam-column goes through the successive stages of  $\varphi_1$  and  $\varphi_2$  and therefore through Case 1, Case 2, and Case 4. For  $q \leq q_{\varphi_m = \varphi_1}$ , the beam-column will behave elastically throughout, and the relation between  $q$  and  $\varphi_m$  is linear (Equation (56)). For  $q > q_{\varphi_m = \varphi_1}$ , there will be a region of the beam-column which will behave plastically. As  $\rho_1$  decreases from  $\ell/2$  to  $\rho_1^l$ , this region will spread through an increasing portion of the beam-column. At any instant in this interval, one can assume a value of  $\rho_1$  and obtain the value of  $x_p$  from Equation (62). With this value of  $x_p$ , the corresponding lateral load  $q$  can be computed from Equation (61) by trial and error. Finally, for  $\rho_1 < \rho_1^l$ , yielding on the lower portion of the beam-column at the center also develops, and Case 4 takes over.

Suppose that the end loadings are large enough to cause part of the beam-column to become plastic on one side before the lateral load  $q$  is applied. Let us assume that this initial plastic zone begins at a distance,  $\rho_1^0$ , say, from the ends. Since the value  $\rho_1^0$  corresponds to  $q = 0$ , the constant  $x_p$  in Equation (61) is  $l/2$ , and thus the value  $\rho_1^0$  can be obtained readily from Equation (62) by trial and error. Again, it is convenient to obtain numerical results by first assuming a value of  $\rho_1$  ( $\rho_1^l \leq \rho_1 \leq \rho_1^0$ ) and obtaining the corresponding value of  $x_p$  from Equation (62) and, therefore, the lateral load  $q$  from Equation (61) by trial and error.

To obtain the curvature curve over the central portion of the beam-column where the cross sections are primary plastic, one simply substitutes the values of constants from Equations (58) and (61) into Equation (37), and the resulting equation is the curvature curve for the primary plastic zone which is expressed implicitly as a function of  $x$

$$\begin{aligned} \frac{x}{l} = & \frac{1}{2} - \frac{\sqrt{c}}{\sqrt{2} \varphi_1^{3/4} \eta^{3/2}} \frac{1}{kl} \left\{ \eta^{1/2} \left[ \frac{\varphi_1}{\varphi} \eta - \left( \frac{\varphi_1}{\varphi} \right)^{1/2} \right]^{1/2} \right. \\ & - \frac{\sqrt{2}\sqrt{c} \varphi_1^{1/4} \eta^{1/2} \left( \frac{\alpha q}{kl} \right)}{c \varphi_1^{1/2} \eta - 2 \left( \frac{\alpha q}{kl} \right)^2} + \tanh^{-1} \left[ 1 - \left( \frac{\varphi}{\varphi_1} \right)^{1/2} \frac{1}{\eta} \right]^{1/2} \\ & \left. - \tanh^{-1} \left[ \frac{\sqrt{2}}{\sqrt{c} \varphi_1^{1/4} \eta^{1/2}} \left( \frac{\alpha q}{kl} \right) \right] \right\} \end{aligned} \quad (65)$$

Valid for

$$\rho_1 \leq x \leq \frac{\ell}{2}$$

9. SOLUTION OF THE ELASTIC-PLASTIC  
BEAM-COLUMN YIELDED ON  
TWO SIDES - CASE 4

Referring to Fig. 1(c) (Case 4) in addition to the primary plastic zone, the secondary plastic zone extends a distance  $\rho_2$  from the ends. The procedure for solving the problem is similar to that used before.

The curvature curve (Equation (57)) for the wholly elastic end portions of the beam-column is still applicable if the appropriate value of  $\rho_1$  is used.

As for the primary plastic zone for which,  $\rho_1 \leq x \leq \rho_2$ , the derivative of the curvature function is given by Equation (34). The constant of integration D in this equation can be determined from the jump condition, as given by Equation (44), for the section where the elastic and primary plastic zones meet. Using the fact that  $\varphi_{x=\rho_1} = \varphi_1$ , it can be concluded that

$$D = \varphi_1^{1/2} \eta \quad (66)$$

The derivative of the curvature function for the secondary plastic zone, for which,  $\rho_2 \leq x \leq l/2$ , is given by Equation (35). The constant G and the unknown curvature,  $\varphi_m$ , at the center of the beam-column can now be determined from the jump condition, as given by Equation (50), for the section where the concentrated load is applied, and the jump condition, as given by Equation (45), for

the section where the primary plastic zone and secondary plastic zone meet. These two conditions together with  $\varphi_{x=\ell/2} = \varphi_m$ , and  $\varphi_{x=\rho_2} = \varphi_2$  give

$$G = \frac{c}{2f} (\varphi_1^{1/2} \eta - \varphi_2^{1/2}) - \frac{1}{\varphi_2} \quad (67)$$

$$\varphi_m = \frac{f}{\left(\frac{\alpha q}{k\ell}\right)^2 + \frac{f}{\varphi_2} - \frac{c}{2} (\varphi_1^{1/2} \eta - \varphi_2^{1/2})} \quad (68)$$

valid for

$$\varphi_m \geq \varphi_2$$

To determine the curvature curve in the primary plastic zone as well as in the secondary plastic zone, the constants of integration  $x_p$  and  $x_s$  in Equations (37) and (38) must be determined. The constants are found from the conditions that  $\varphi$ , as given by Equations (37) and (38), must equal  $\varphi_1$  for  $x = \rho_1$  and must equal  $\varphi_m$  for  $x = \ell/2$ , respectively.

Substituting the values of  $x_p$  and  $x_s$  thus obtained into Equations (37) and (38), respectively, yields the curvature curve expressed implicitly as a function of  $x$  for these two zones. Using the relations given in Equation (67) and Equation (68), it follows that

$$\frac{x}{\ell} = \frac{\rho_1}{\ell} + \frac{\sqrt{c}}{\sqrt{2}} \frac{1}{\eta^{3/2} \varphi_1^{3/4}} \frac{1}{k\ell} \left\{ \eta^{1/2} (\eta-1)^{1/2} - \left[ \frac{\eta^2 \varphi_1}{\varphi} - \frac{\eta \varphi_1^{1/2}}{\varphi^{1/2}} \right]^{1/2} \right. \\ \left. + \tanh^{-1} \left( 1 - \frac{1}{\eta} \right)^{1/2} - \tanh^{-1} \left[ 1 - \frac{\varphi^{1/2}}{\eta \varphi_1^{1/2}} \right]^{1/2} \right\} \quad (69)$$

valid for

$$\rho_1 \leq x \leq \rho_2$$

and

$$\frac{x}{\ell} = \frac{1}{2} - \frac{2}{3} \frac{\sqrt{f}}{k\ell} \left\{ \left[ \frac{c}{2f} \left( \varphi_1^{1/2} \eta - \varphi_2^{1/2} \right) - \frac{1}{\varphi_2} + \frac{1}{\varphi} \right]^{1/2} \left[ \frac{2}{\varphi_2} + \frac{1}{\varphi} \right. \right. \\ \left. \left. - \frac{c}{f} \left( \varphi_1^{1/2} \eta - \varphi_2^{1/2} \right) \right] - \frac{1}{\sqrt{f}} \left( \frac{\alpha q}{k\ell} \right) \left[ \frac{1}{f} \left( \frac{\alpha q}{k\ell} \right)^2 \right. \right. \\ \left. \left. + \frac{3}{\varphi_2} - \frac{3c}{2f} \left( \varphi_1^{1/2} \eta - \varphi_2^{1/2} \right) \right] \right\} \quad (70)$$

valid for

$$\rho_2 \leq x \leq \frac{\ell}{2}$$

in which  $\eta$  is a function of the as yet unknown distance  $\rho_1$ , as defined in Equation (60). The unknown distances,  $\rho_1$  and  $\rho_2$ , which denoted elastic-primary plastic and primary-secondary plastic boundaries,

respectively, can now be determined from the conditions at the section  $x = \rho_2$ . At this section, the two portions of the curvature curve, as given by Equation (69) and Equation (70), have a common value and must equal  $\varphi_2$ . After some algebraic manipulation, one obtains

$$\begin{aligned} \frac{\rho_2}{\ell} = \frac{\rho_1}{\ell} + \frac{\sqrt{c}}{\sqrt{2}} \frac{1}{\eta^{3/2} \varphi_1^{3/4}} \frac{1}{k\ell} \left\{ \eta^{1/2} (\eta-1)^{1/2} - \left[ \frac{\varphi_1}{\varphi_2} \eta^2 - \frac{\varphi_1^{1/2}}{\varphi_2^{1/2}} \eta \right]^{1/2} \right. \\ \left. + \tanh^{-1} \left( 1 - \frac{1}{\eta} \right)^{1/2} - \tanh^{-1} \left[ 1 - \frac{\varphi_2^{1/2}}{\varphi_1^{1/2}} \frac{1}{\eta} \right]^{1/2} \right\} \quad (71) \end{aligned}$$

and also the desired equation for the elastic-primary plastic boundary

$\rho_1$

$$\begin{aligned} \left( \frac{\alpha q}{k\ell} \right)^3 + 3 \left[ \frac{f}{\varphi_2} - \frac{c}{2} \left( \varphi_1^{1/2} \eta - \varphi_2^{1/2} \right) \right] \left( \frac{\alpha q}{k\ell} \right) + 3f \\ \left\{ \frac{k\ell}{4} - \frac{k\rho_2}{2} + \frac{\sqrt{c}}{3\sqrt{2}} \left( \varphi_1^{1/2} \eta - \varphi_2^{1/2} \right)^{1/2} \left[ \frac{c}{f} \left( \varphi_1^{1/2} \eta - \varphi_2^{1/2} \right) - \frac{3}{\varphi_2} \right] \right\} = 0 \quad (72) \end{aligned}$$

in which  $\rho_2$  is also a function of  $\rho_1$ .

It is seen that this equation is a cubic equation in  $q$  (or  $\alpha q/k\ell$ ) and the analytical solutions of this equation can be found directly. At the same time the solution for the unknown distance  $\rho_1$  is much more complicated since this quantity enters into hyperbolic functions containing  $\rho_1$  and a method of trial and error

must be utilized in order to obtain a solution. Therefore, it is convenient to obtain numerical results by first solving this equation for  $q$  expressed as a function of  $\rho_1$ . Then, by assuming a value of  $\rho_1$ , the corresponding value of  $q$  can be obtained. Once this is done the corresponding values of the physical characteristics of the beam-column can be computed in a rather straightforward manner.

For simplification the two coefficients of this cubic equation are denoted by  $s$  and  $t$ , respectively, and then Equation (72) becomes

$$\left(\frac{\alpha q}{k\ell}\right)^3 + s \left(\frac{\alpha q}{k\ell}\right) + t = 0 \quad (73)$$

Solving Equation (73) for  $q$ , one obtains

$$q = \frac{k\ell}{\alpha} \left\{ \left[ -\frac{t}{2} + \left(\frac{t^2}{4} + \frac{s^3}{27}\right)^{1/2} \right]^{1/3} + \left[ -\frac{t}{2} - \left(\frac{t^2}{4} + \frac{s^3}{27}\right)^{1/2} \right]^{1/3} \right\} \quad (74)$$

if

$$\frac{t^2}{4} + \frac{s^3}{27} > 0$$

and

$$\begin{aligned} q_1 &= 2 \frac{k\ell}{\alpha} \left(-\frac{t}{2}\right)^{1/3} \\ q_2 &= -\frac{k\ell}{\alpha} \left(-\frac{t}{2}\right)^{1/3} \end{aligned} \quad (75)$$



if

$$\frac{t^2}{4} + \frac{s^3}{27} = 0$$

and

$$\begin{aligned} q_1 &= 2 \frac{k\ell}{\alpha} \left(-\frac{s}{3}\right)^{1/2} \cos \frac{\Psi}{3} \\ q_2 &= 2 \frac{k\ell}{\alpha} \left(-\frac{s}{3}\right)^{1/2} \cos \left(\frac{\Psi}{3} + 120^\circ\right) \\ q_3 &= 2 \frac{k\ell}{\alpha} \left(-\frac{s}{3}\right)^{1/2} \cos \left(\frac{\Psi}{3} + 240^\circ\right) \end{aligned} \quad (76)$$

if

$$\frac{t^2}{4} + \frac{s^3}{27} < 0$$

in which  $\Psi$  is defined as

$$\cos \Psi = -\frac{t}{2} / \left(-\frac{s^3}{27}\right)^{1/2} \quad (77)$$

in which  $s$  and  $t$  present themselves as functions of the parameter

$\rho_1$ .

For a given value of  $\rho_1$  there will exist one (Equation (74)), two (Equation (75)), or three (Equation (76)) real roots for the lateral load  $q$ , possibly. Each root of  $q$  will give a value of  $\varphi_m$ .

The values of  $q$  and  $\varphi_m$  so obtained can either be positive or negative. The negative sign of the value  $q$  indicates that  $q$  acts opposite to the direction assumed in Fig. 1, but can produce either positive or negative curvature at the central portion of the beam-column. However, if one considers only the particular case of positive  $q$  and positive  $\varphi_m$ , then the solution for  $q$ , satisfying such conditions, will be unique, and the unique value of  $q$  will be given by  $q_1$ .

Values of  $\rho_2$  must lie between the limits  $\ell/2$  and  $\rho_2^\ell$  (as yet undefined,  $\rho_2^\ell \geq 0$ ). The value  $\ell/2$  corresponds to  $\varphi_m = \varphi_2$ , the value of  $q$  is given by Equation (64), and the corresponding upper limit value of  $\rho_1$  is  $\rho_1^u$ , which is, of course, equal to the lower limit value of  $\rho_1^\ell$  obtained already in Case 2. When the curvature  $\varphi_m$ , as given by Equation (68), approaches infinity the plastic regions in the upper and lower portions of the beam-column meet at the center and a so-called plastic hinge forms, and the value of  $q$  is

$$q_{\varphi_m \rightarrow \infty} = \frac{k\ell}{\alpha} \left[ \frac{c}{2} \left( \varphi_1^{1/2} \eta - \varphi_2^{1/2} \right) - \frac{f}{\varphi_2} \right]^{1/2} \quad (77)$$

and the corresponding lower limit value,  $\rho_1^\ell$ , of  $\rho_1$ , and therefore the lower limit value,  $\rho_2^\ell$ , can readily be found from Equation (72) by trial and error.

Again, as discussed in Section 8, it is possible that the end loadings may be large enough to cause part of the

beam-column to become plastic on two sides already before the lateral load  $q$  is applied. In such circumstances the initial upper limit value of  $\rho_2$  will be  $\rho_2^0$  instead of the value  $\ell/2$ . The value of  $\rho_1^0$ , which corresponds to  $q = 0$  (or  $\rho_2 = \rho_2^0$ ), can be obtained from Equation (72) by equating  $q$  to zero and by using a method of trial and error. Values of  $\rho_1$  must now lie between the limits  $\rho_1^0$  and  $\rho_1^\ell$  and the values of  $\rho_2$  must lie between  $\rho_2^0$  and  $\rho_2^\ell$ . The lateral load  $q$  corresponding to  $\rho_1 = \rho_1^0$  is zero. The load  $q$  corresponding to  $\rho_1 = \rho_1^\ell$  is given by Equation (77). For other values of  $q$  Equations (74), (75), and (76) can be used readily by assuming various values of  $\rho_1$ .

## 10. NUMERICAL RESULTS

### Interaction Curves

A complete numerical evaluation of this solution for the beam-column problem has been performed on a CDC 6400 Digital Computer. The results of calculations made with various individual cases are calculated for structural steel with  $E = 30,000$  ksi and  $\sigma_y = 34$  ksi.

The desired  $(q, \varphi_m)$ -curve can be obtained directly from various individual cases. A typical plot of  $q$  versus  $\varphi_m$  for a beam-column of given eccentricity ratio  $e/r$  and slenderness ratio  $\ell/r$ , subjected to the constant load  $p$ , is shown in Fig. 6 in which values of  $e/r = 1$ ,  $\ell/r = 40$ , and  $p = 0.2, 0.4$  have been used. The small circles and the dotted lines in the figure indicate the different stages of plastification within the beam-column. It is known that for any given axial force  $p$  it is necessary to increase the lateral load  $q$  at the beginning in order to produce an increase of mid-section curvature, while beyond a certain limit, given by the maximum point of the curve, further curvature may proceed with a diminishing of the load. Although the diminishing of the load with respect to an increase in curvature is not seen for the curve  $p = 0.2$  (within the range of  $\varphi$  less than 10) and is not rapid for the curve  $p = 0.4$  as shown in Fig. 6, it is observed, however, that when the slenderness ratio of the beam-column and/or the axial compressive force are increased, there is a rapid diminishing portion of the curve beyond the maximum point. Thus the maximum points of

the curves in Fig. 6 represent, for the given slenderness ratio and assumed eccentricity, the maximum strength of the beam-column.

The maximum loads obtained in this way for various values of axial force  $p$ , slenderness ratio  $\ell/r$ , and assumed eccentricity ratio  $e/r$  are represented by the interaction curves in Figs. 7 to 10. The curves are drawn for values of  $\ell/r$  from 20 to 160 and each graph is plotted for a value of  $e/r$  and a particular cross section. For each value of  $e/r$  (0 and 0.5), two sets of such curves are shown, one for  $R = 0$  valid for a solid rectangular cross section, and the other for  $R = 1.4$ , valid for a wide-flange cross section (8 W 31). The dotted-open circle curves in Fig. 7 to Fig. 10 represent the dividing lines between the range of applicability of various individual cases. Each curve is for a particular beam-column and gives the combinations of axial force and lateral load that can be safely supported by the beam-column. Since the interaction curves are nondimensionalized, they can be directly used in analysis and design computations.

The interaction curves determined by the analytical solutions for an eccentrically loaded column are compared in Fig. 11 with those obtained previously by Galambos and Ketter [13] using the method of numerical integration. It can be seen that, in general, the values of the maximum strength computed from the approximate  $m-\phi-p$  curve (Fig. 3) is lower than the values determined from the real  $m-\phi-p$  curve (except the curve  $\ell/r = 20$  in the lower axial force range), but the difference is usually small. This is expected because

the approximate  $m-\phi-p$  curves in Fig. 3 generally underestimate the real curves. It should be noted, however, that the interaction curves of the present analytical solutions are based on 0.05  $p$  intervals while the curves obtained by numerical integration are generally based on 0.2  $p$  [13]. Therefore, part of the discrepancy probably results from such difference in plotting.

It was shown in Section 4 that the generalized  $m-\phi-p$  expressions generally tend to overestimate the actual moment when the value of  $R$  is assumed to be 1 (Fig. 4,  $\phi \geq 1.1$ ) and to underestimate when the value of  $R$  is assumed to be 1.4 (Fig. 3). Thus the maximum loads of a beam-column computed from the value  $R = 1$  will be an upper bound on the actual maximum load. The maximum loads computed from  $R = 1.4$  will be a lower bound. In Figs. 12 and 13 are shown two sets of interaction curves of this kind calculated for  $e/r = 0, 0.5$ , respectively. It can be seen that the interaction curves are relatively insensitive to minor variations in  $R$ , especially for beam-columns with high slenderness ratio. It may be concluded from this comparison that the interaction curves derived here for a particular value of  $R$ , for example  $R = 1.4$ , may be used for the analysis of all wide-flange beam-column sections (on conservative side for 8 W 31 section).

It was shown in Section 4 that for a given cross section and a given axial force, the constants which specify the generalized  $m-\phi-p$  relationship will be known from Equations (16) to (28).

Assuming that the axial force  $p$  is maintained at a constant value, it can be seen from the solutions of the preceding sections that the functional relationship between the lateral load  $q$  and the mid-section curvature  $\phi_m$  only involves two independent parameters  $e/r$  (or  $m_0$ ) and  $k\ell$ . The parameter  $k\ell$  is of importance in the analysis and design of beam-column, because it enables the interaction curves prepared for one yield stress level to be used for different yield stress levels. Since the axial force  $p$  is assumed to remain constant for a particular beam-column problem, the parameter  $k\ell$  becomes a function of the two ratios:  $\sigma_y/E$  and  $\ell/r$

$$k\ell = \sqrt{\frac{p \sigma_y}{E}} \left(\frac{\ell}{r}\right) \quad (78)$$

As long as the value for the parameter  $k\ell$  remains the same, the  $(q, \phi_m)$ -curves corresponding to different combinations of  $\sigma_y/E$  and  $\ell/r$  will be identical for any assumed eccentricity ratio. Thus the interaction curves, prepared here for steel with a yield stress of 34 ksi, can be applied to steels of other yield stress levels by simply substituting an equivalent slenderness ratio

$$\left(\frac{\ell}{r}\right)_{\text{equ}} = \sqrt{\frac{34}{\sigma_y}} \left(\frac{\ell}{r}\right) \quad (79)$$

Here  $E$  is assumed to be the same for all different yield stress steels.

This conclusion is identical with that of Reference 14.

### Initial Curvature

If an initially curved beam-column with an initial curvature  $\varphi_0^*$  is submitted to the action of an axial force  $p$  and a distributed lateral load  $w(x)$ , additional curvatures  $\varphi_1^*$  will be produced so that the final ordinates of the curvature curve are

$$\varphi = \varphi_0^* + \varphi_1^* \quad (80)$$

and the equation of equilibrium for bending of the beam-column is, in the usual notation

$$\frac{d^2 m}{dx^2} + k^2 (\varphi_0^* + \varphi_1^*) = - \frac{w}{M_y} \quad (81)$$

or

$$\frac{d^2 f(\varphi_1^*)}{dx^2} + k^2 \varphi_1^* = - \frac{w}{M_y} - k^2 \varphi_0^* \quad (82)$$

where  $f(\varphi)$  denotes the functional relationship between bending moment  $m$  and curvature  $\varphi$  for a given axial force  $p$ .

It can be seen that the differential equation for the curvature curve  $\varphi_1^*$  of the initially curved beam-column is of the same form and has the same boundary conditions as that of a straight beam-column but with an additional lateral load  $k^2 \varphi_0^*$ . Therefore, the problem of bending of an initially curved beam-column can be approached



by the concept of replacing the effect of initial curvature on the curvatures by the effect of an equivalent lateral load of the intensity  $k^2 \varphi_0^*$ . The dimensional form of the expression for the intensity of the equivalent lateral load is  $P \Phi_0^*$  which is obtained by multiplying the dimensionless value  $k^2 \varphi_0^*$  by  $M_y$  and using the notation  $k^2 = P \Phi_y / M_y$ .

In the previous discussions, one considered a very general case of an inelastic beam-column with initial curvature and distributed lateral load. The particular case of an elastic column compressed by force  $p$  applied at the ends has been discussed thoroughly by Timoshenko [1].

As an example, assume that the initial shape of the beam-column consists of two equal straight-line portions, as shown by dotted line in Fig. 14, with a maximum deflection at the middle equal to  $y_0$ . The equivalent lateral load becomes a concentrated load  $Q$  at the middle span. The magnitude of the equivalent lateral load is obtained from the above expression

$$Q = \int_0^l P \Phi_0^* dx = \int P d\theta_0^* = 4P \left( \frac{y_0}{l} \right) \quad (83)$$

where  $\theta_0^*$  denotes the slope of the initial shape of the beam-column, or in nondimensional form the equivalent lateral load has the form

$$q = \left( \frac{p}{2\alpha} \right) \left( \frac{h}{r} \right)^2 \left( \frac{y_0}{h} \right) \quad (84)$$

Through the use of the equivalent lateral load concept, the effect of this curvature on the maximum strength of a beam-column can be readily obtained from the interaction curves similar to those in Figs. 7 to 10. Since the ratio of the cross section depth to the radius of gyration as well as the shape factor of a cross section depend on the shape of the cross section, the above equivalent lateral load will also depend on the shape of the cross section. Take rectangular cross section, for example, the values of  $h/r$  and  $\alpha$  are  $2\sqrt{3}$  and 1.5, respectively. If the initial deflection ratio  $y_0/h$  of the beam-column is assumed to be  $1/20$ , say, then the value of the equivalent lateral load, as given by Equation (84), will be  $q = 0.2 p$ . The straight line  $q = 0.2 p$  is drawn in Fig. 7, and the points of intersection of this line with the various interaction curves give the maximum strength of the column when it is loaded with the specified initial curvature. The results obtained are shown in Fig. 14 for several values of the initial curvature  $y_0/h$ . The curve with the small circles in Fig. 14 are plotted as corresponding small circles in Fig. 7 for the particular value of  $y_0/h = 1/20$ .

In column design it was pointed out [1] that it is logical to assume that the initial curvature of a column may be compensated for by a certain eccentricity in the application of the axial force. In Fig. 15 three sets of such curves are compared, calculated for a solid rectangular cross section. It is assumed that the values

of initial curvature are independent of the length of the column. The comparison shows that the initial imperfections of a column can be compensated for with sufficient accuracy by a certain eccentricity.

### Curvature Curves

The curvature curves obtained in the previous sections may be plotted in a single diagram for various values of  $q$ . Figure 16 shows a family of such curves with  $e/r = 1$ ,  $\ell/r = 60$ , and  $p = 0.3$ . The extent of the elastic, primary plastic and secondary plastic zones of the beam-column corresponding to different stages of loading,  $q$ , are denoted by heavy solid lines, dotted lines, and light solid lines, respectively, in the figure. These curves were computed for beam-column with a rectangular cross section and again with material properties  $\sigma_y = 34$  ksi and  $E = 30,000$  ksi.

Knowing the values of curvature along the elastic-plastic beam-column, the lateral load vs. end slope or the lateral load vs. mid-span deflection can be readily obtained through the use of the following two expressions

$$\theta_{x=0} = \frac{2 \left( \frac{\sigma_y}{E} \right) \left( \frac{\ell}{r} \right)}{\left( \frac{h}{r} \right)} \int_0^{0.5} \frac{\Phi}{\Phi_y} d \left( \frac{x}{\ell} \right) \quad (85)$$

$$\frac{y_{x=\ell/2}}{h} = \frac{2 \left( \frac{\sigma_y}{E} \right) \left( \frac{\ell}{r} \right)^2}{\left( \frac{h}{r} \right)^2} \int_0^{0.5} \left( \frac{\Phi}{\Phi_y} \right) \left( \frac{x}{\ell} \right) d \left( \frac{x}{\ell} \right) \quad (86)$$

As an example, taking the curvature curves as shown in Fig. 16 as the basis for computations, the corresponding lateral load vs. end slope curve is shown in Fig. 17 in which point 1 corresponds to the value of load  $q = 0.053$  at which the yield point is just reached in the most compressed fiber of the mid-section of the beam-column; point 2 corresponds to the value of  $q = 0.292$  for which the fiber of maximum tensile stress of the mid-section on the convex side of the beam-column has also reached its yield point, and the maximum value of the curve for  $q$  is 0.371 which defines the maximum strength of the beam-column.

To see the rate of expansion of the plastic zones as the end slope increases, the distances  $\rho_1$  and  $\rho_2$  which specify the elastic-primary plastic boundary as well as the primary-secondary plastic boundary, respectively, are also plotted against the end slope in Fig. 17. It is seen that the initial rate of expansion of the plastic zone on the compressive side of the beam-column (see curve marked  $\rho_1$ ) is very rapid and this rate falls steadily, and the curve for  $\rho_1$  bends over more and more as the end slope increases. When the end slope reaches the value approximately 0.025 radians the value of  $\rho_1$  becomes practically a constant and equals the value 0.093  $\ell$ . The curve for  $\rho_2$  is very similar to the curve of  $\rho_1$ , but the initial rate of plastic expansion on the tensile side is less rapid and the value of  $\rho_2$  practically approaches the constant 0.328  $\ell$  when the end slope reaches the value approximately 0.0275 radians.

From this discussion it can be concluded that when the load  $q$  is gradually increased to its maximum and then drops off steadily beyond the maximum point, the plastic zones spread first toward the ends of the beam-column with a high initial rate of expansion with respect to the rate of expansion toward the axis of the beam-column. Beyond a certain value of  $q$ , further end rotation may proceed with mainly expanding the plastic zones toward the axis of the beam-column while the expansion toward the ends has practically ceased. In the limit the plastic regions in the upper and lower portions of the beam-column will meet at the center and a so-called plastic hinge forms.

## 11. CONCLUSIONS

An analytical solution that describes the elastic-plastic behavior of an eccentrically loaded beam-column under a concentrated load at the mid-span was obtained. In the analysis, the moment-curvature-thrust relationships derived previously for a rectangular section are generalized to represent any complex shape of structural section to a high degree of approximation. Furthermore, curvature instead of deflection was utilized to simplify greatly the mathematical aspect of the problem. It is shown how the load-curvature curves of beam-columns can be obtained directly from the solution. The interaction curves for the applied lateral load versus axial force with various values of slenderness ratio and eccentricity ratio of the beam-column at the instant of collapse was obtained from the load-curvature curves.

## 12. ACKNOWLEDGEMENTS

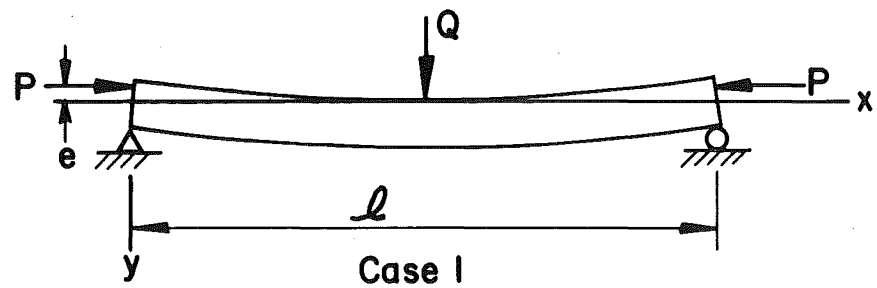
The work is a part of the general investigation on "Space Frames with Biaxial Loading in Columns", currently being carried out at the Fritz Engineering Laboratory, Lehigh University. This study is sponsored jointly by the Welding Research Council and the Department of the Navy, with funds furnished by the American Iron and Steel Institute, Naval Ships System Command, and Naval Facilities Engineering Command.

Technical advice for the project is provided by the Lehigh Project Subcommittee of the Structural Steel Committee of the Welding Research Council, of which T. R. Higgins is Chairman.

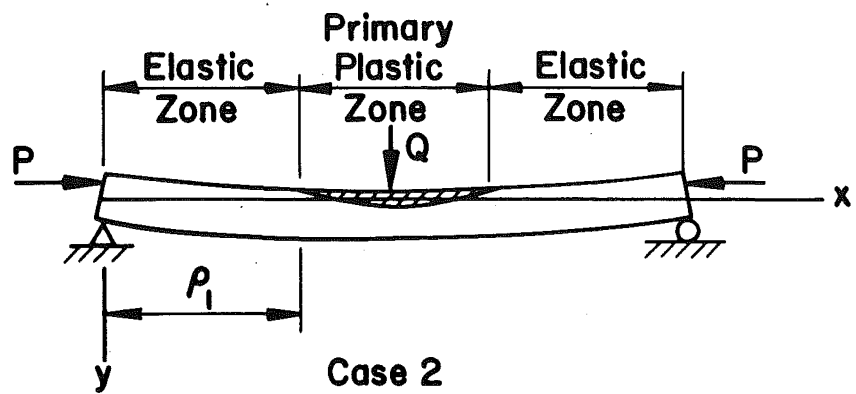
The writer wishes to acknowledge S. N. Iyengar for his help in computer programming, to L. W. Lu and G. C. Driscoll for their review of the manuscript, to J. Lenner for her help in typing the manuscript, and to J. Gera for preparing the drawings.

### 13. FIGURES

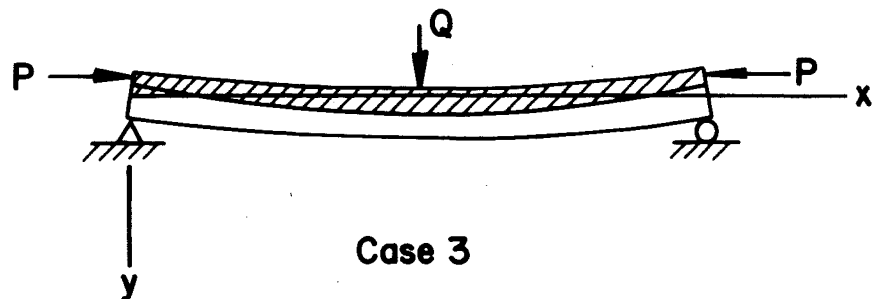




(a) Elastic



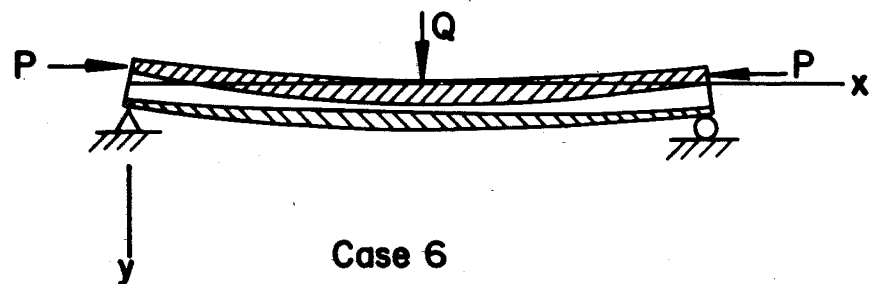
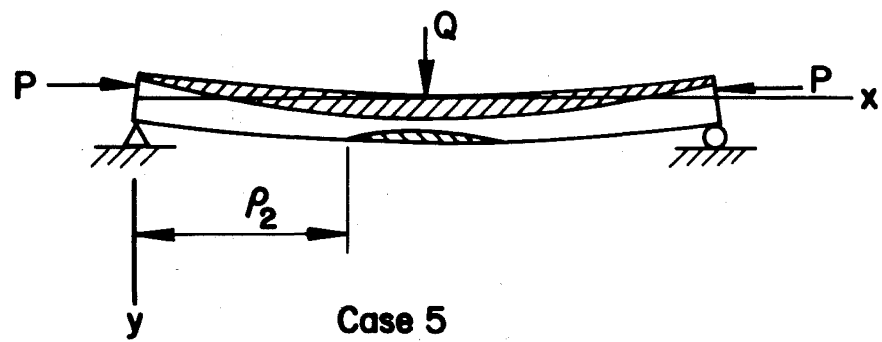
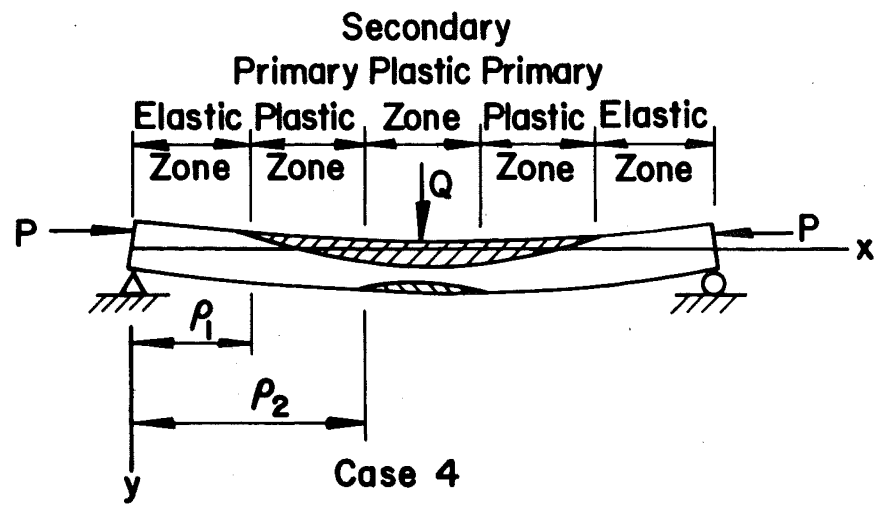
Case 2



Case 3

(b) One Side Plastic

Fig. 1 Eccentrically Loaded Beam-Column



(c) Two-Side Plastic

Fig. 1 Eccentrically Loaded Beam-Column (Contd.)

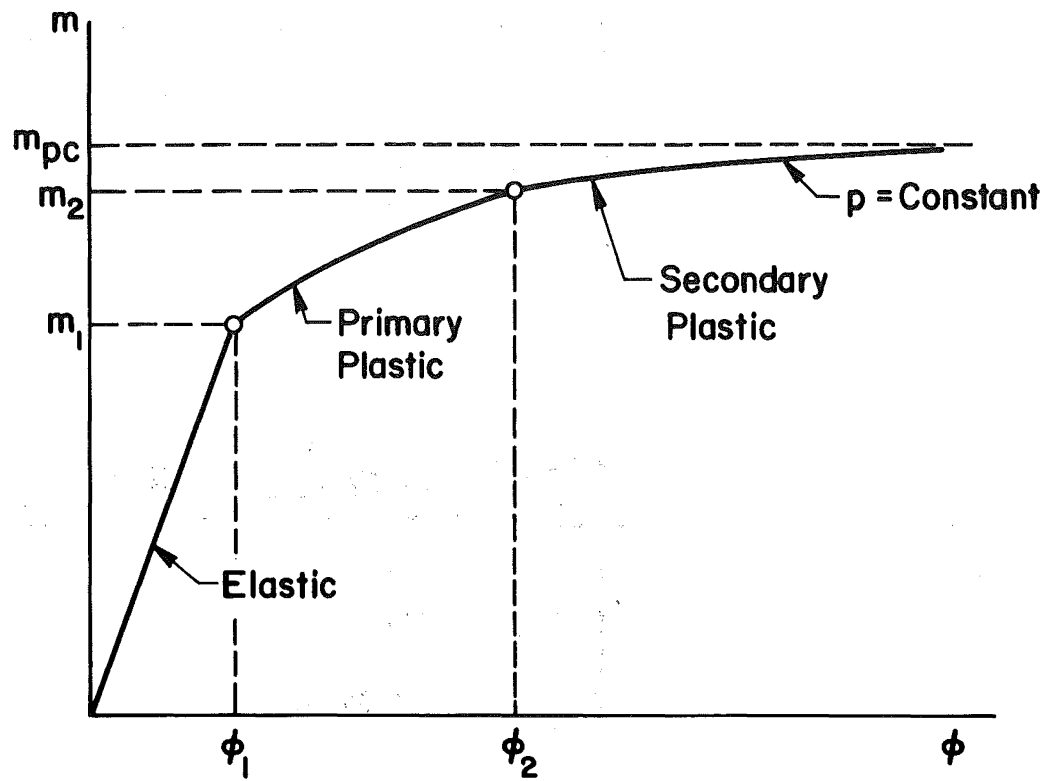


Fig. 2 Moment-Curvature-Thrust Relationship for a Common Structural Section

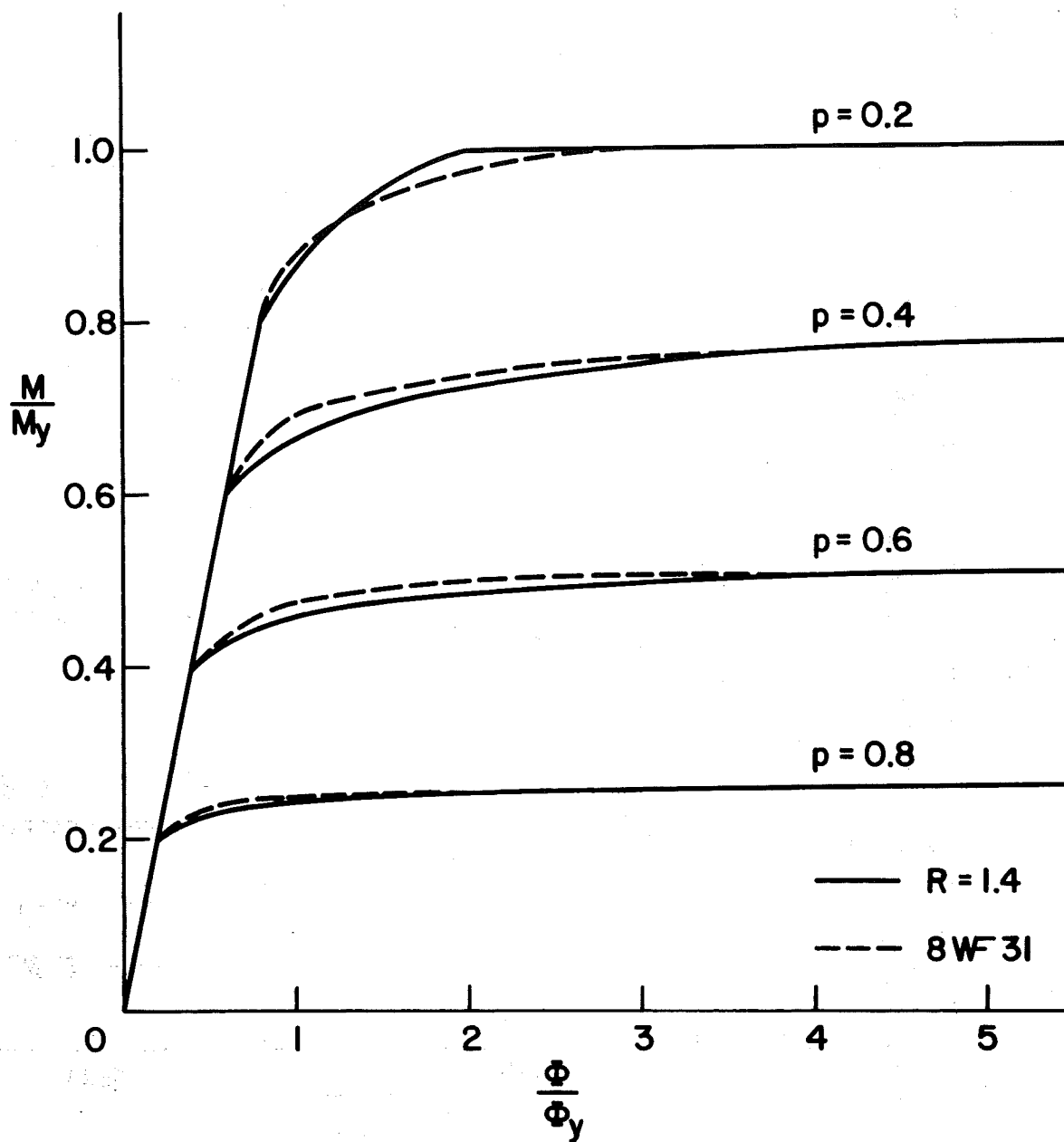


Fig. 3 Moment-Curvature-Thrust Relationships  
(Actual Curves Shown Dashed)

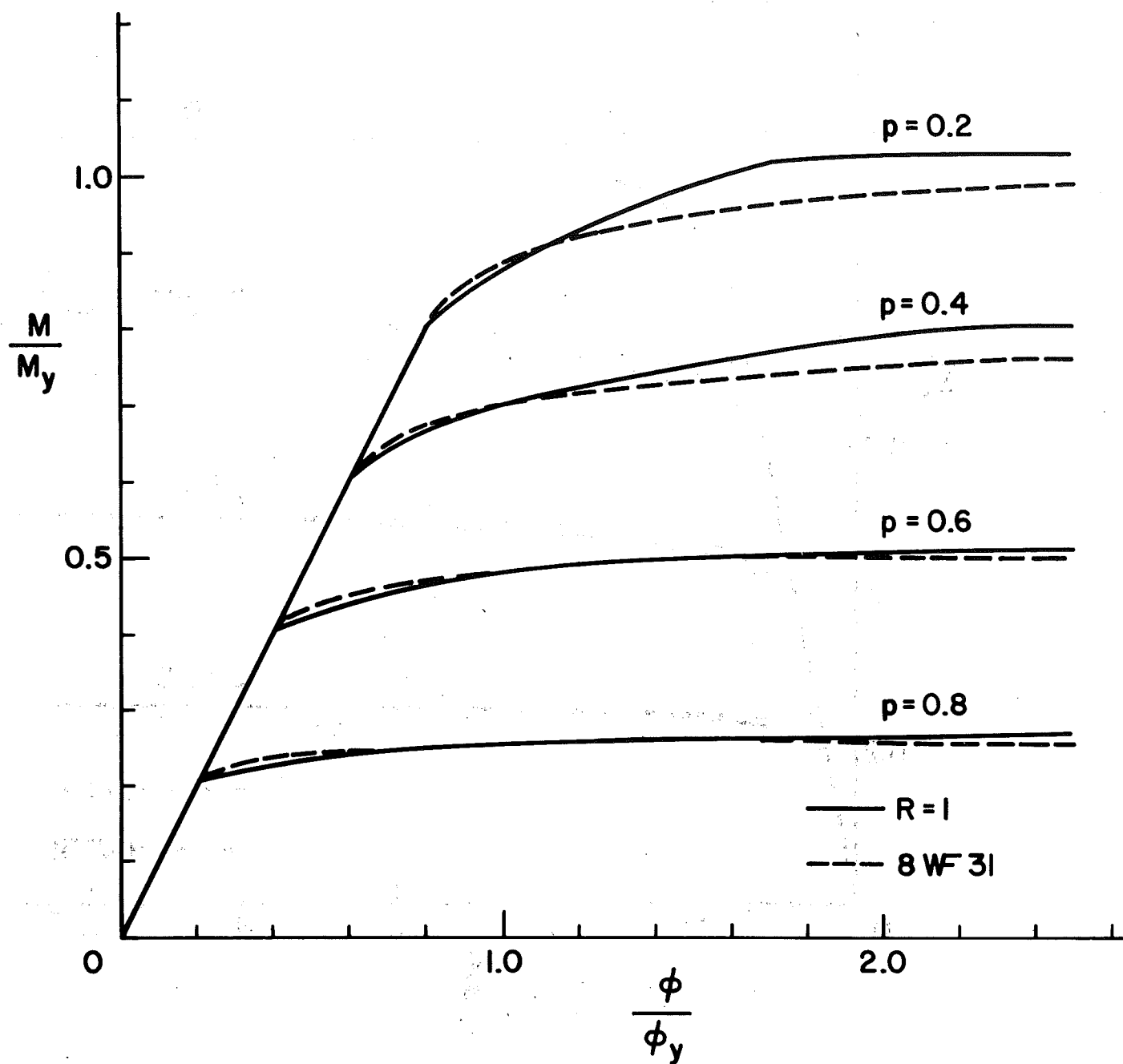


Fig. 4 Moment-Curvature-Thrust Relationships  
(Actual Curves Shown Dashed)

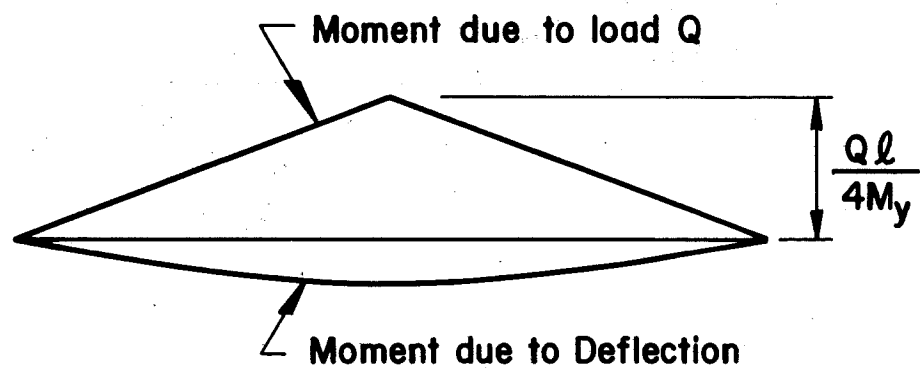
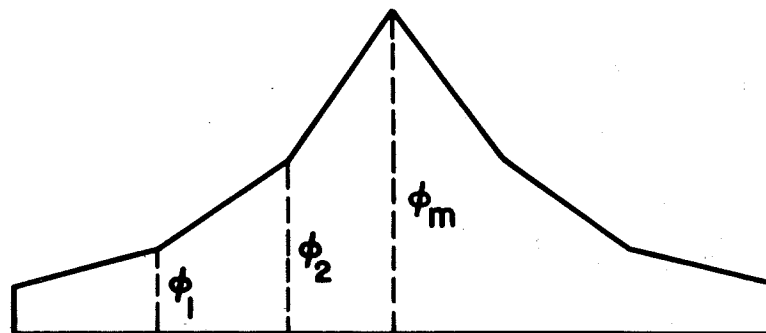
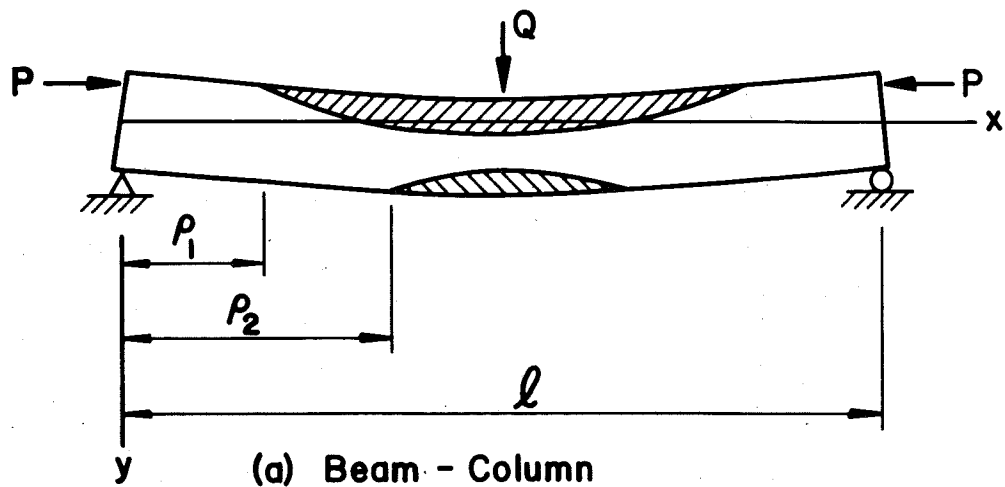


Fig. 5 Discontinuities in the Derivative of the Curvature Curve

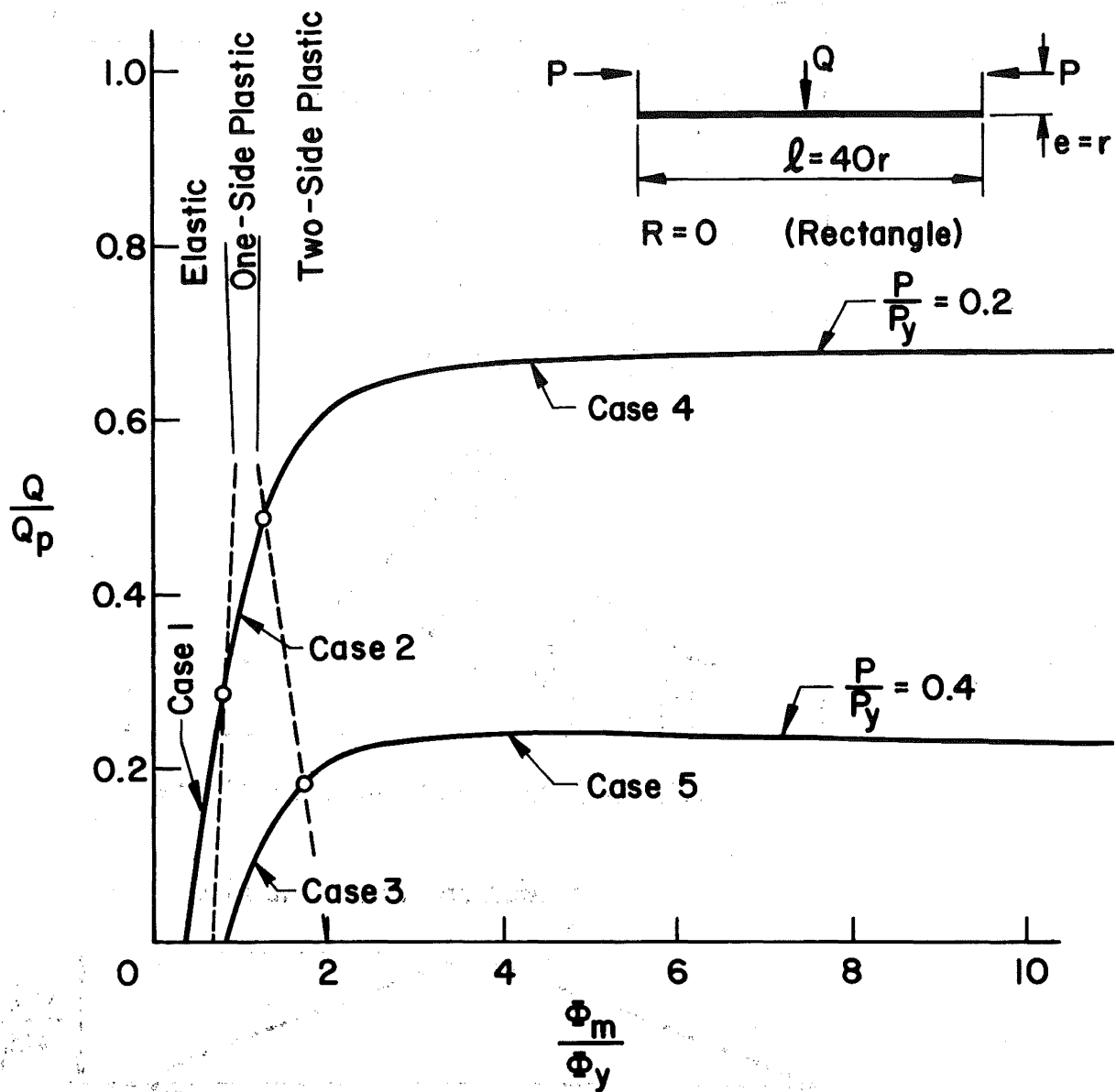


Fig. 6 Lateral Load vs. Mid-Section Curvature Curves.  $E = 30,000$  ksi,  $\sigma_y = 34$  ksi

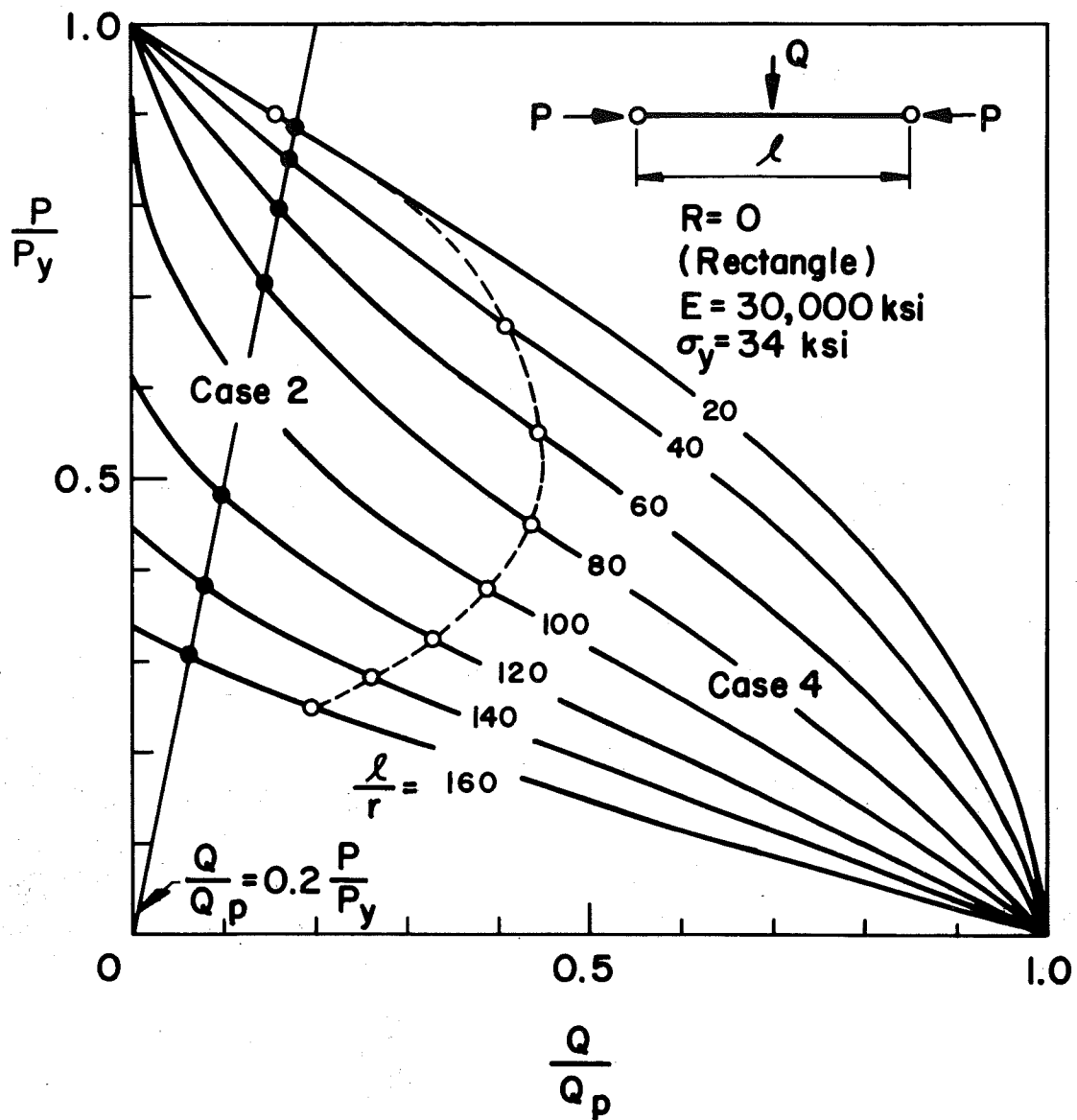


Fig. 7 Interaction Curves for a Rectangular Cross Section



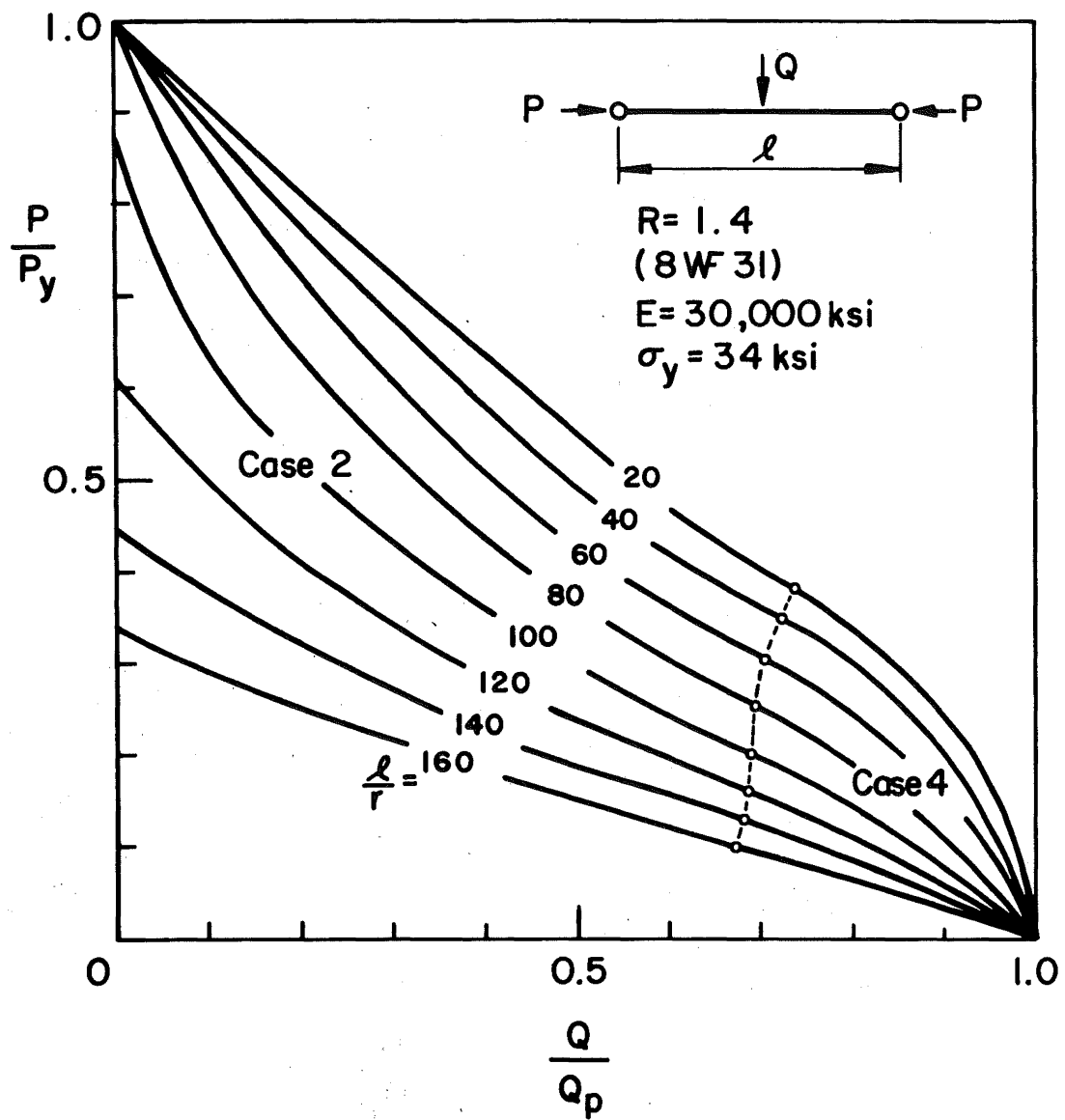


Fig. 8 Interaction Curves for a Wide-Flange Cross Section

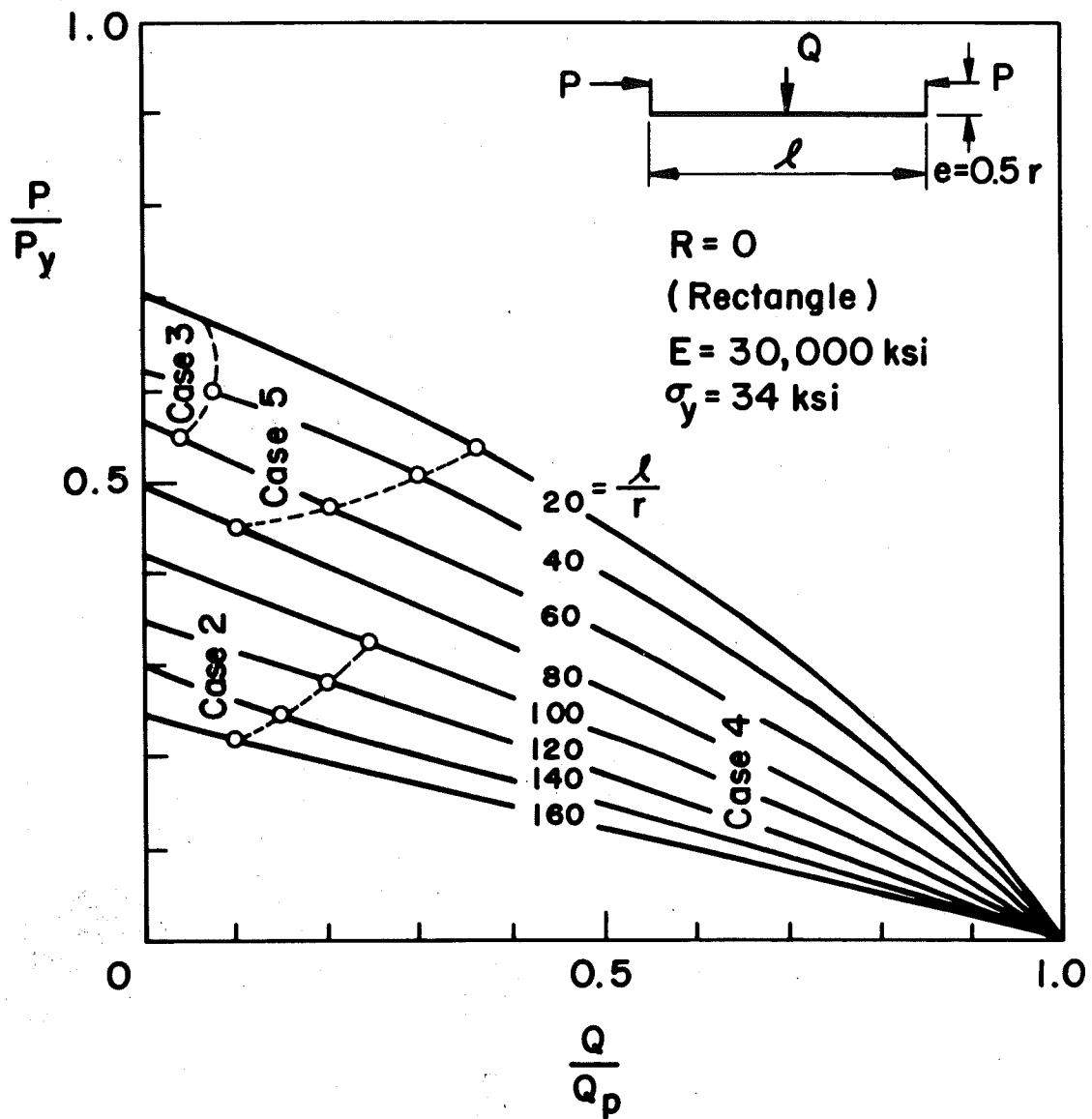


Fig. 9 Interaction Curves for a Rectangular Cross Section with a Constant Eccentricity

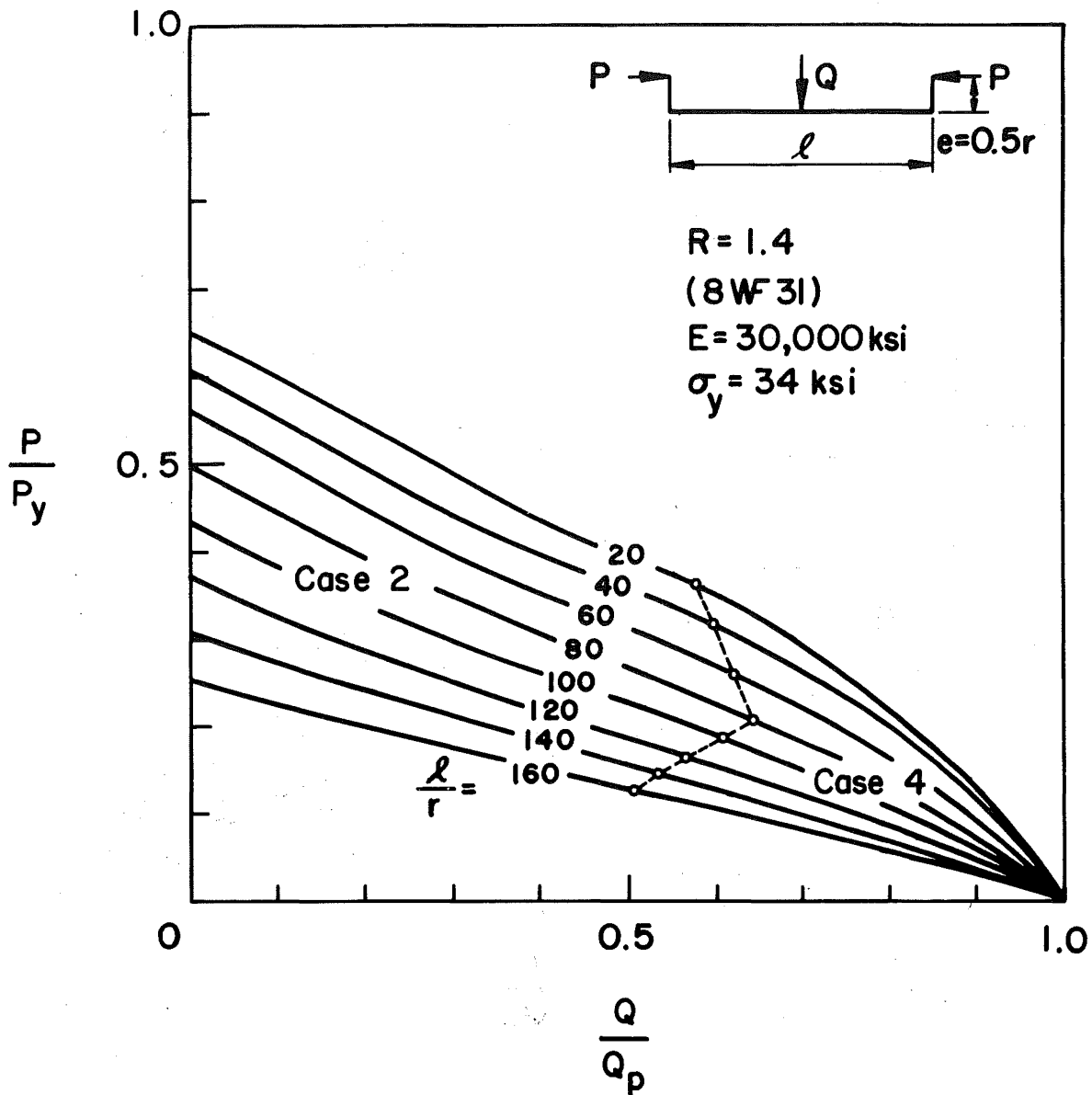


Fig. 10 Interaction Curves for a Wide-Flange Cross Section with a Constant Eccentricity

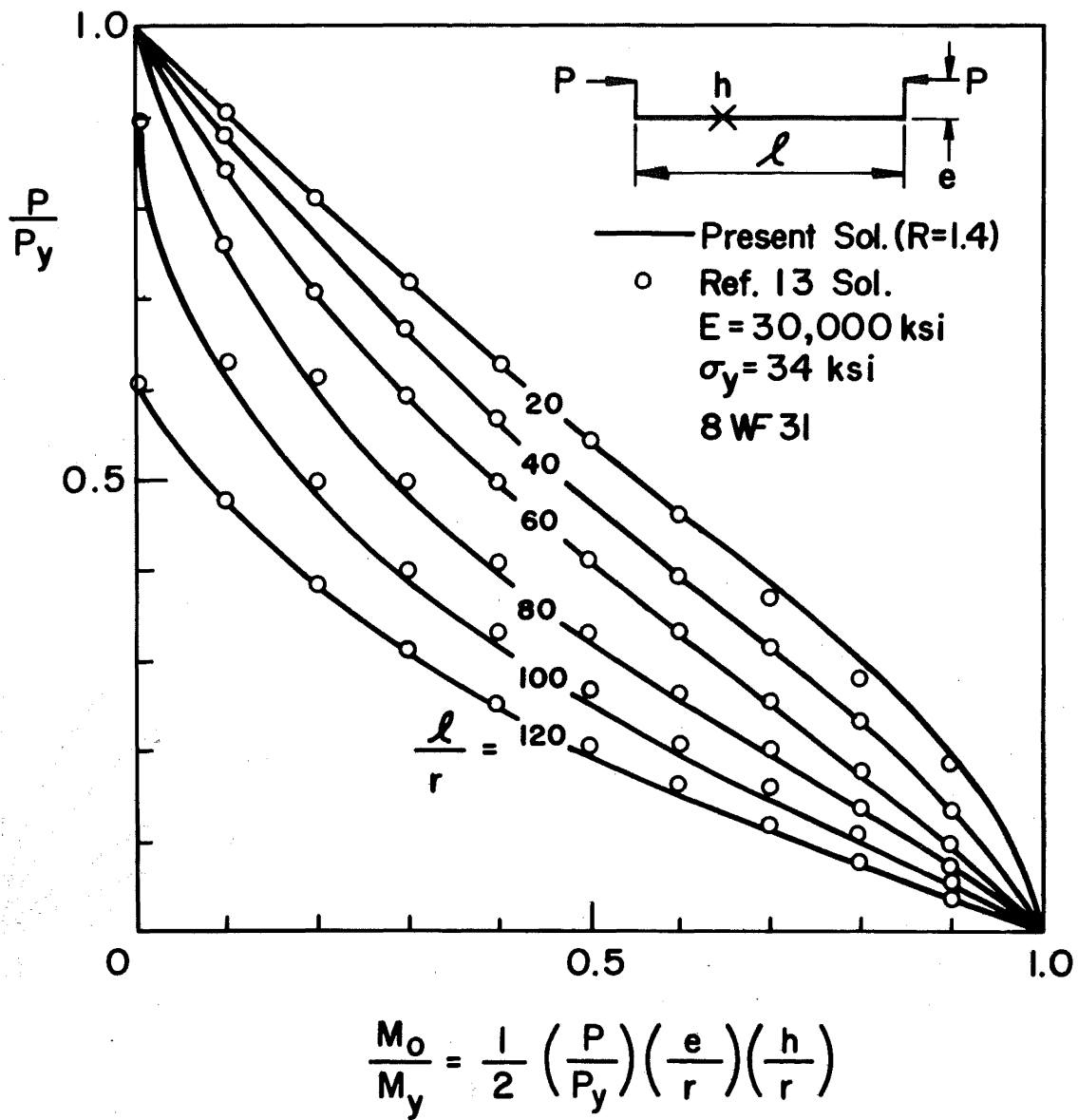


Fig. 11 Comparison Between "Analytical" and "Numerical" Interaction Curves

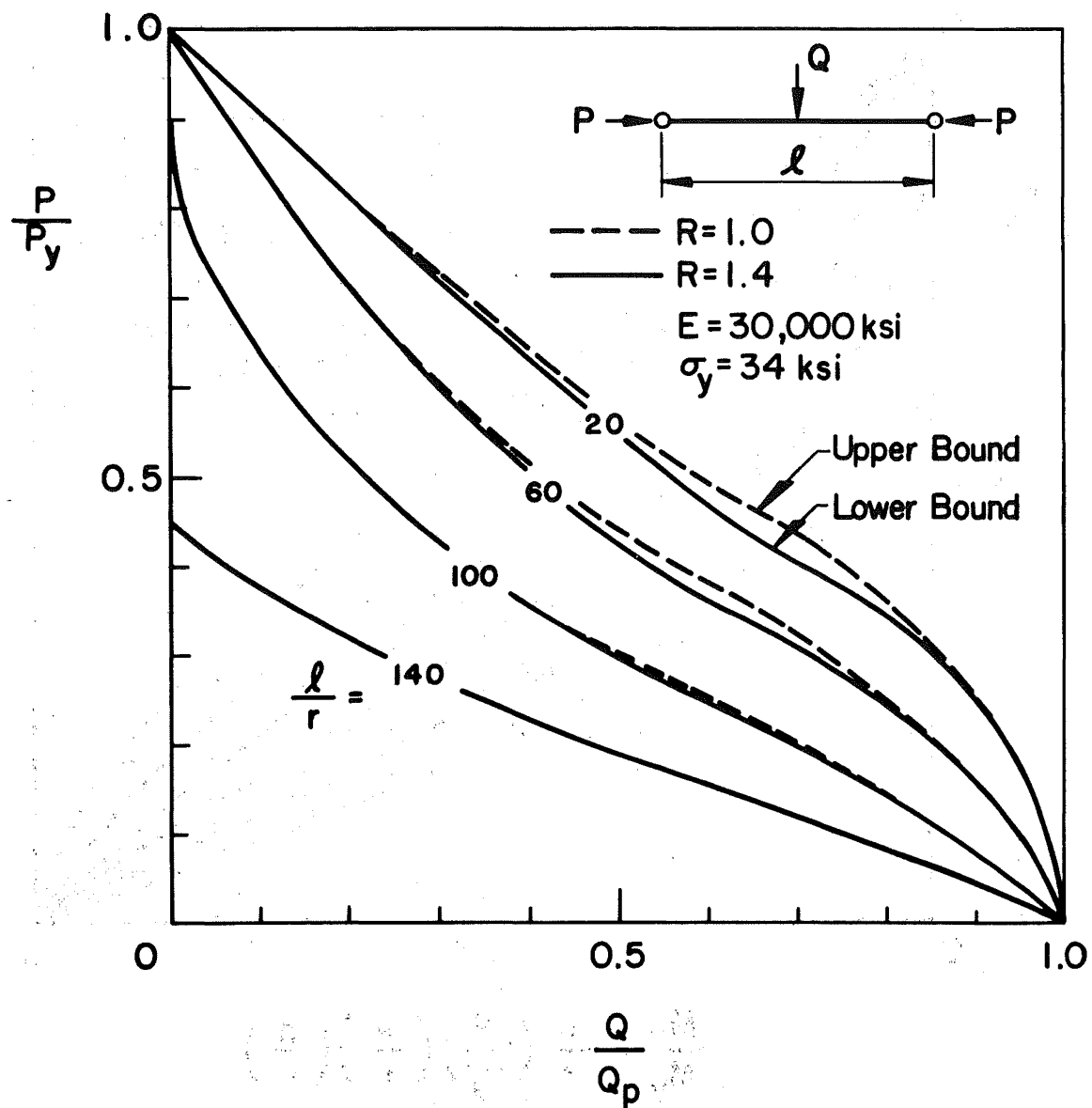


Fig. 12 Comparison of Lower and Upper Bounds  
for the Ultimate Strength of an  
Axially Loaded Beam-Column

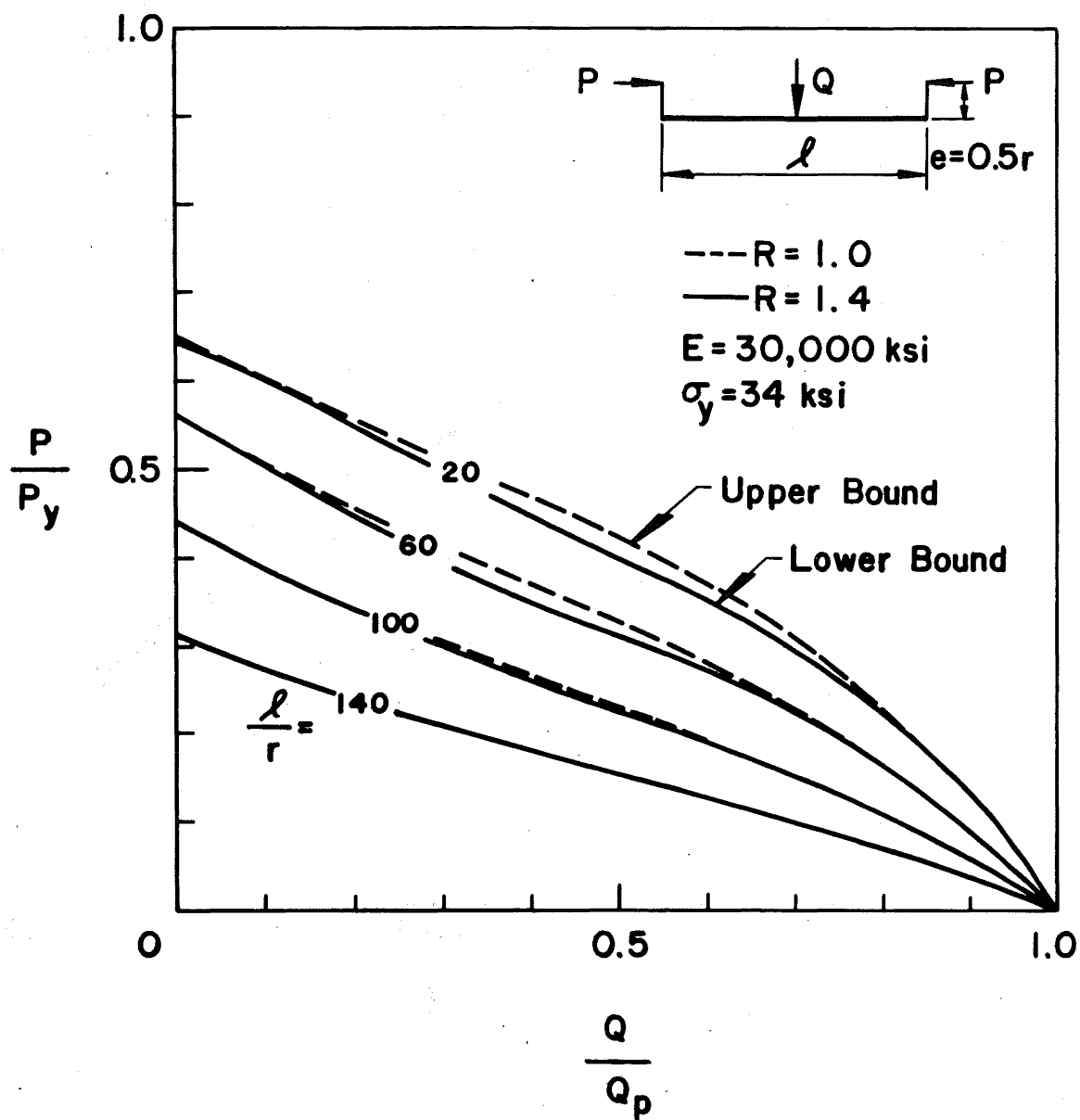


Fig. 13 Comparison of Lower and Upper Bounds for the Ultimate Strength of an Eccentricity Loaded Beam-Column

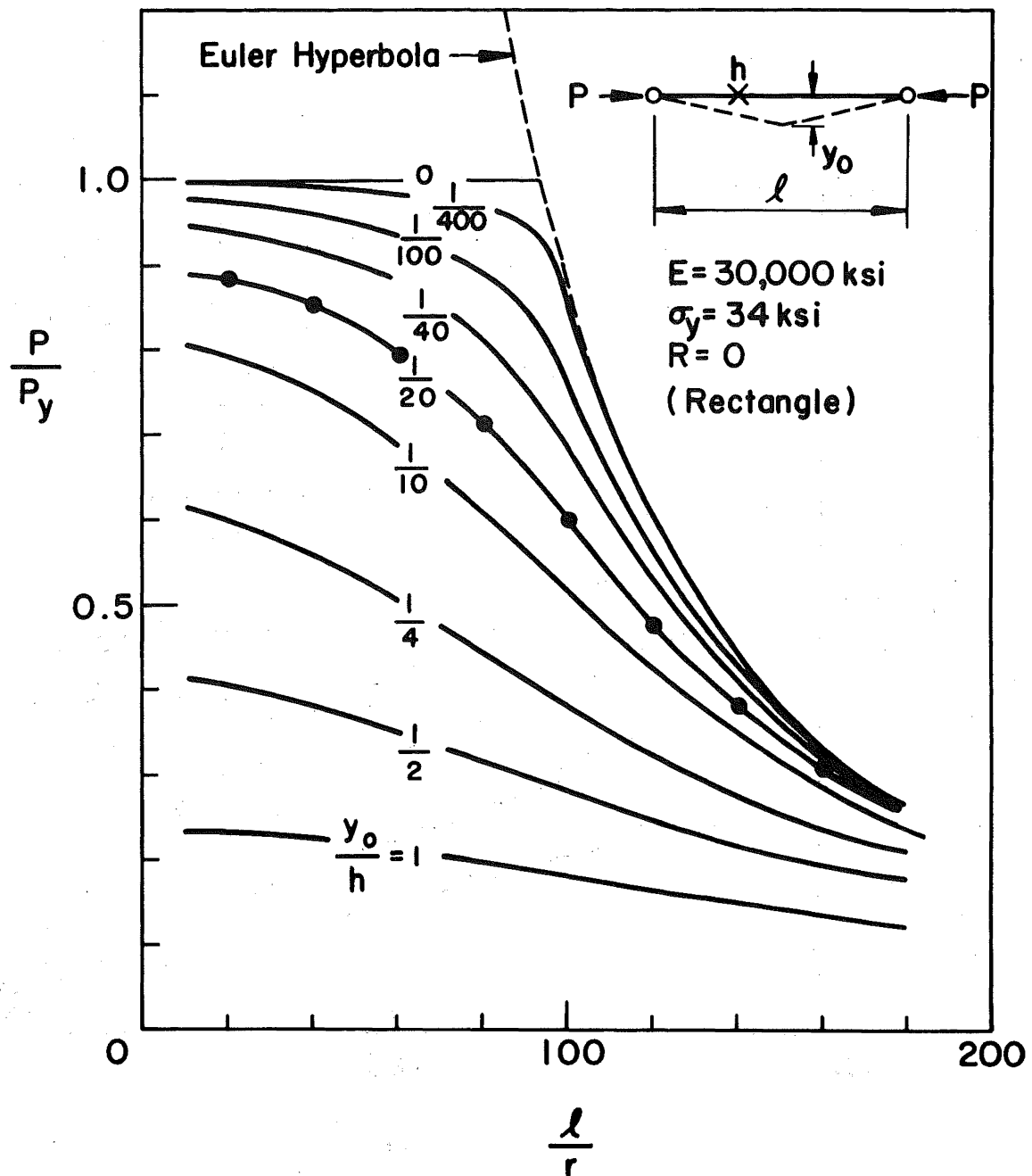


Fig. 14 The Effect of Initial Curvature on the Ultimate Strength of a Column

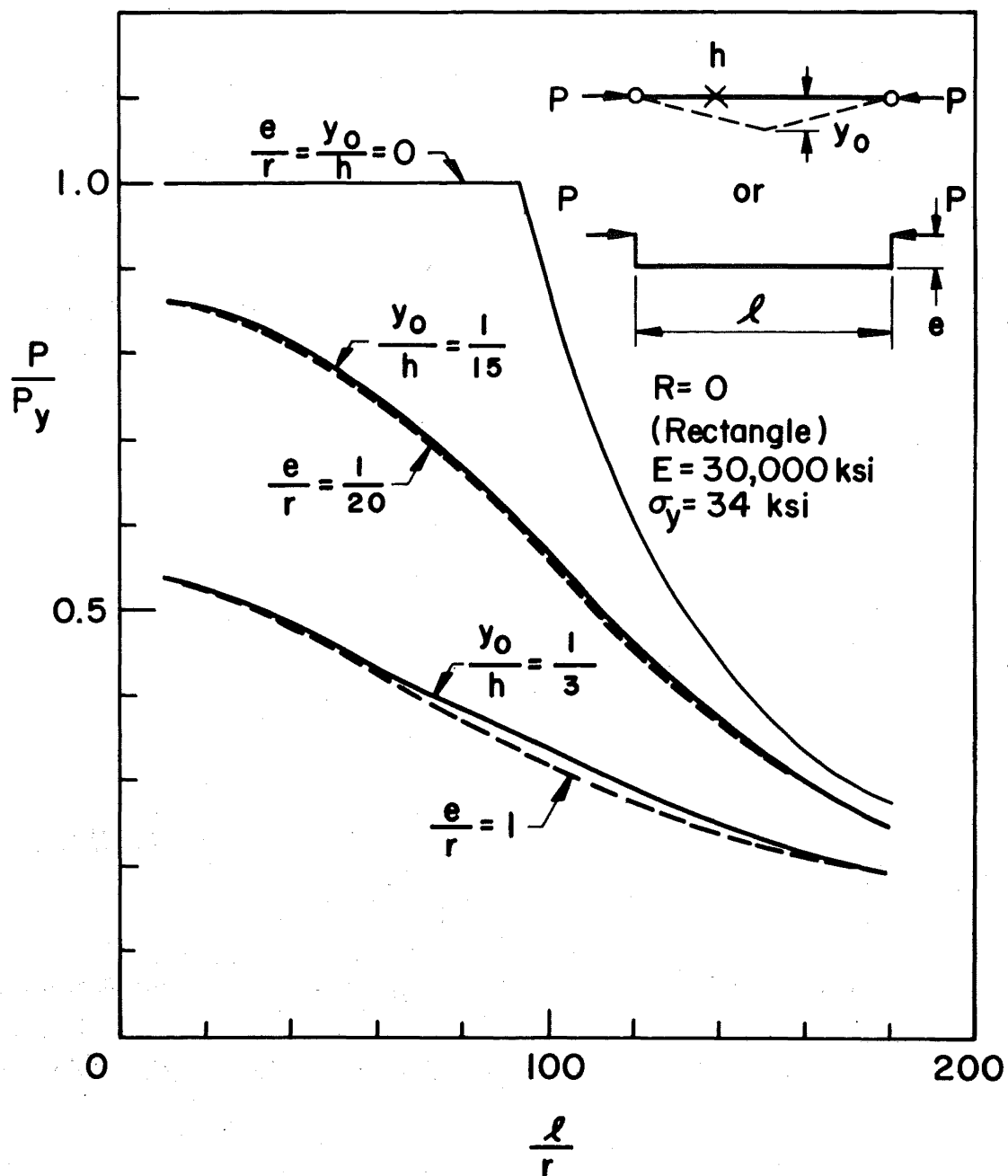


Fig. 15 Comparison of Column Curves for a Column with Initial Imperfections and for a Column with Initial End Eccentricities



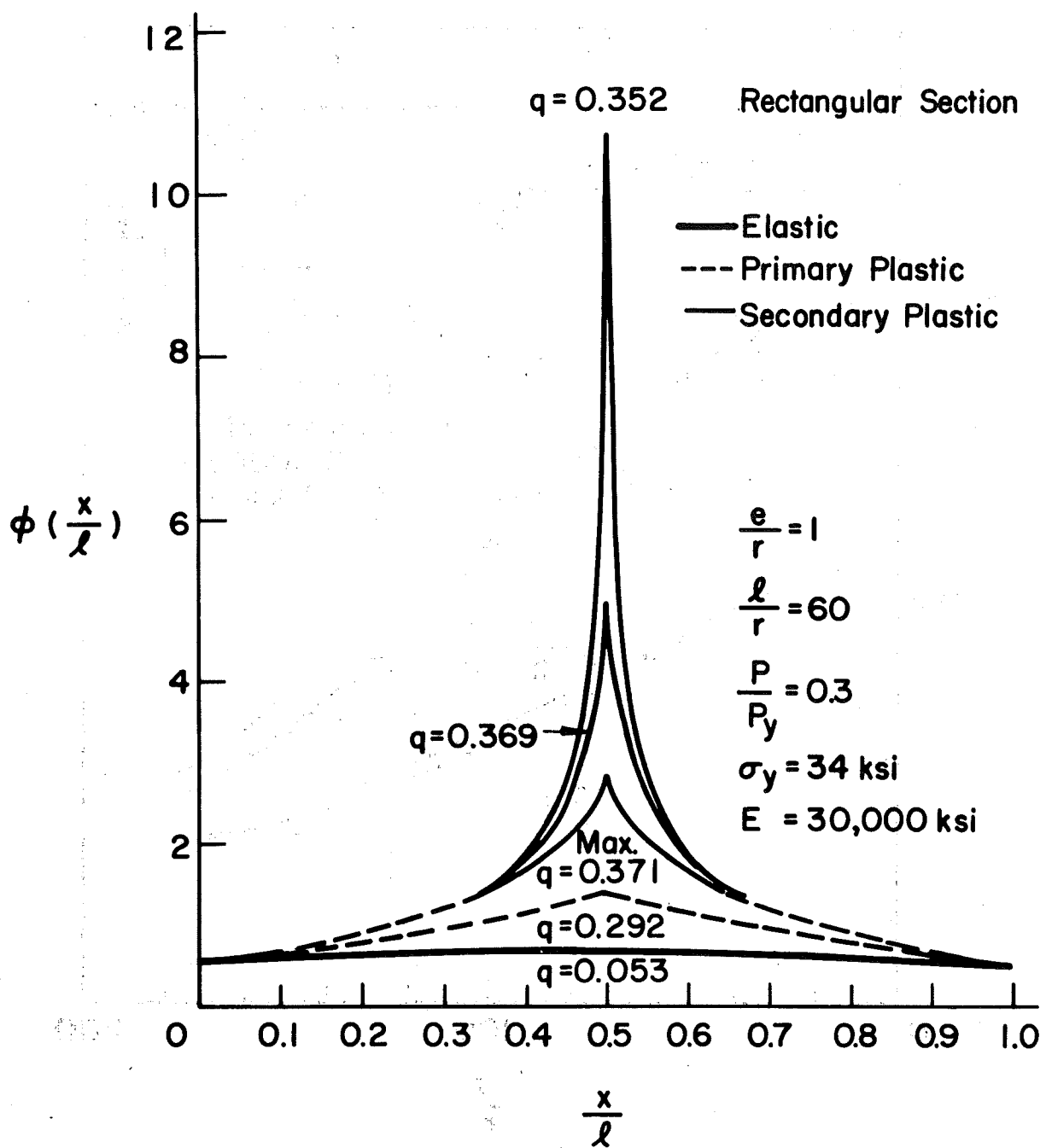


Fig. 16 Curvatures along the Length of a Beam-Column

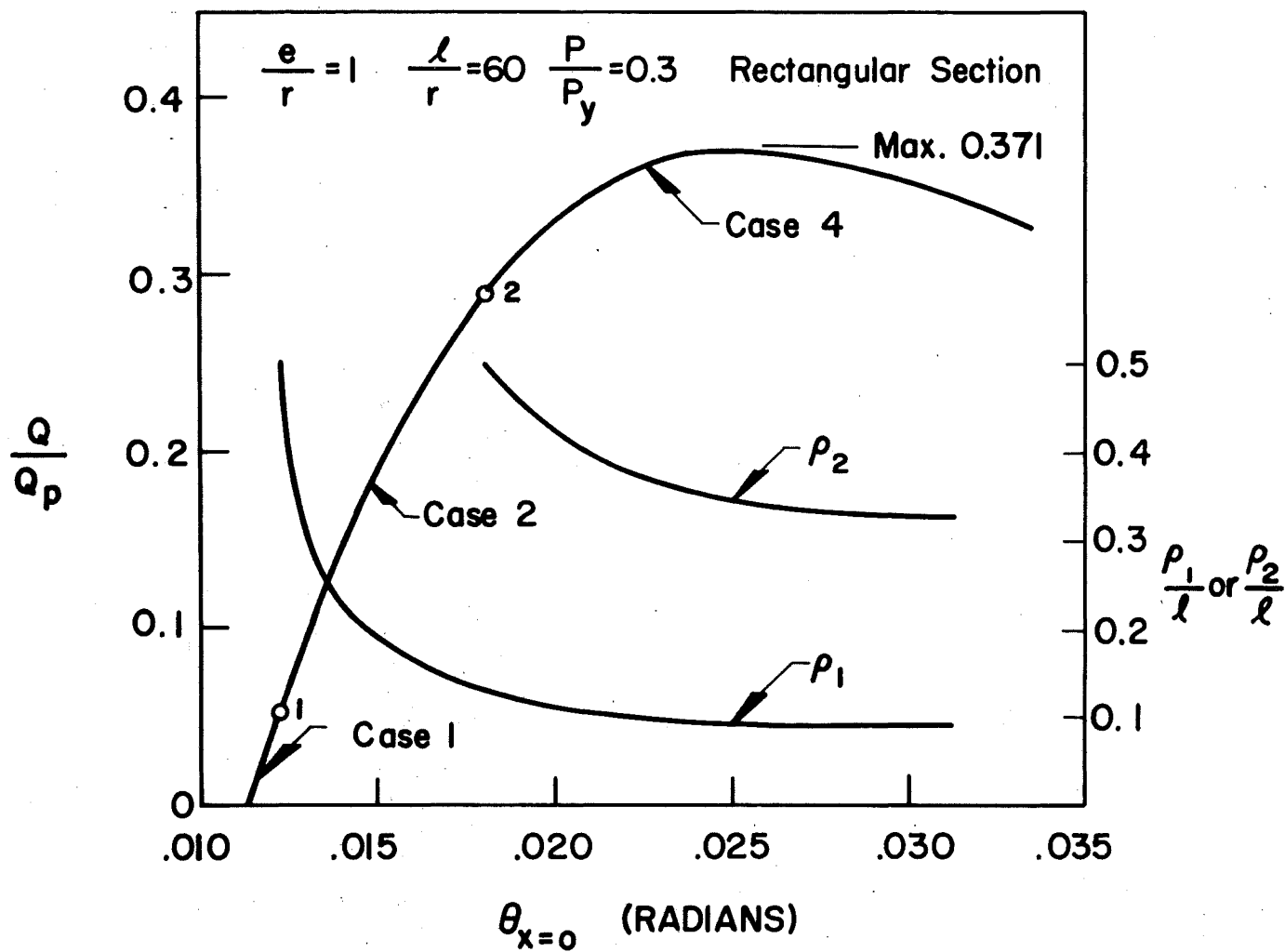


Fig. 17 Lateral Load vs. End Slope Curve and the Corresponding Values for  $\rho_1$  and  $\rho_2$

## APPENDICES

### 14. APPENDIX I - SOLUTION FOR CASE 3, CASE 5, AND CASE 6

Case 3 [Fig. 1(b)] - The general solution of the curvature curve of this case is given by Equation (37). The constant D is found from the condition that  $d\varphi/dx$  in Equation (34) must satisfy the "jump condition", as given by Equation (49). Hence

$$D = \varphi_m^{1/2} + \frac{2}{c} \left( \frac{\alpha q}{k\ell} \right)^2 \quad (87)$$

The constant  $x_p$  and the unknown quantity  $\varphi_m$  can be determined from the conditions that  $\varphi$  in Equation (37) must equal  $\varphi_m$  and  $\varphi_0$  for  $x = \ell/2$  and  $x = 0$ , respectively. One obtains

$$\frac{x_p}{\ell} = \frac{1}{2} + \frac{1}{D} \frac{1}{k\ell} \left\{ \left( \frac{\alpha q}{k\ell} \right) \frac{1}{\varphi_m^{1/2}} + \frac{\sqrt{c}}{\sqrt{2}} \frac{1}{D^{1/2}} \tanh^{-1} \left[ \frac{\sqrt{2}}{\sqrt{c}} \frac{1}{D^{1/2}} \left( \frac{\alpha q}{k\ell} \right) \right] \right\} \quad (88)$$

and the desired equation for the determination of the unknown curvature  $\varphi_m$  at the central cross section of the beam-column

$$k\ell = \frac{\sqrt{2c}}{D^{3/2}} \left\{ D^{1/2} \left[ \frac{(D - \varphi_0)^{1/2}}{\varphi_0^{1/2}} - \frac{\sqrt{2}}{\sqrt{c}} \frac{1}{\varphi_m^{1/2}} \left( \frac{\alpha q}{k\ell} \right) \right] + \tanh^{-1} \left[ 1 - \frac{\varphi_0}{D} \right]^{1/2} - \tanh^{-1} \left[ \frac{\sqrt{2}}{\sqrt{c}} \left( \frac{\alpha q}{k\ell} \right) \frac{1}{D^{1/2}} \right] \right\} \quad (89)$$

where

$$\varphi_0 = \frac{c^2}{(b-m_0)^2} \quad (90)$$

valid for

$$\varphi_1 \leq \varphi_0 \leq \varphi_2$$

and

$$\varphi_1 \leq \varphi_m \leq \varphi_2$$

Case 5 [Fig. 1(c)] - The derivatives of the curvature function for the primary plastic zone and for the secondary plastic zone are given by Equation (34) and Equation (35), respectively. The constants D and G are found from the jump condition, as given by Equation (50), for the central cross section where the concentrated load is applied, and also the jump condition, as given by Equation (45), for the section where the primary plastic zone and secondary plastic zone meet. Using the fact that  $\varphi_{x=l/2} = \varphi_m$ , and  $\varphi_{x=p_2} = \varphi_2$ , it can be concluded that

$$D = \varphi_2^{1/2} + \frac{2f}{c\varphi_2} \left[ 1 - \frac{\varphi_2}{\varphi_m} + \frac{\varphi_2}{f} \left( \frac{\alpha q}{k\ell} \right)^2 \right] \quad (91)$$

$$G = \frac{1}{f} \left( \frac{\alpha q}{k\ell} \right)^2 - \frac{1}{\varphi_m}$$

To determine the curvature curve in the secondary plastic zone, the constant  $x_s$  in Equation (38) and the unknown distance  $\rho_2$  must be determined. The values  $x_s$  and  $\rho_2$  are found from the conditions that  $\varphi$ , as given by Equation (38), must equal  $\varphi_2$  for  $x = \rho_2$  and must equal  $\varphi_m$  for  $x = l/2$ , respectively. One obtains

$$\frac{x_s}{l} = \frac{1}{2} - \frac{2}{kl} \left( \frac{\alpha q}{kl} \right) \left[ \frac{2}{3f} \left( \frac{\alpha q}{kl} \right)^2 - \frac{1}{\varphi_m} \right] \quad (92)$$

and

$$\begin{aligned} \frac{\rho_2}{l} = \frac{1}{2} - \frac{2}{3} \frac{\sqrt{f}}{kl} \left[ \frac{1}{f} \left( \frac{\alpha q}{kl} \right)^2 + \frac{1}{\varphi_2} - \frac{1}{\varphi_m} \right]^{1/2} \left[ \frac{1}{\varphi_2} + \frac{2}{\varphi_m} - \frac{2}{f} \left( \frac{\alpha q}{kl} \right)^2 \right] \\ + \frac{2}{kl} \left( \frac{\alpha q}{kl} \right) \left[ \frac{1}{\varphi_m} - \frac{2}{3f} \left( \frac{\alpha q}{kl} \right)^2 \right] \end{aligned} \quad (93)$$

To determine the curvature curve in the primary plastic zone, the constant  $x_p$  in Equation (37) and the unknown quantity  $\varphi_m$  must be determined. The values  $x_p$  and  $\varphi_m$  are found from the conditions that  $\varphi$ , as given by Equation (37), must equal  $\varphi_0$  for  $x = 0$  and must equal  $\varphi_2$  for  $x = \rho_2$ , respectively. One obtains

$$\frac{x_p}{l} = \frac{\sqrt{c}}{\sqrt{2}} \frac{1}{kl} \frac{1}{D} \left\{ \frac{(D - \varphi_0)^{1/2}}{\varphi_0^{1/2}} + \frac{1}{D^{1/2}} \tanh^{-1} \left[ 1 - \frac{\varphi_0^{1/2}}{D} \right]^{1/2} \right\} \quad (94)$$

in which  $\varphi_0$  is given by Equation (90) and the desired equation for the unknown curvature  $\varphi_m$  at the central cross section of the beam-column

$$\begin{aligned}
\frac{k\ell}{2} = & \frac{2\sqrt{f}}{3} \left[ \frac{1}{\varphi_2} - \frac{1}{\varphi_m} + \frac{1}{f} \left( \frac{\alpha q}{k\ell} \right)^2 \right]^{1/2} \left[ \frac{1}{\varphi_2} + \frac{2}{\varphi_m} - \frac{2}{f} \left( \frac{\alpha q}{k\ell} \right)^2 \right] \\
& - 2 \left( \frac{\alpha q}{k\ell} \right) \left[ \frac{1}{\varphi_m} - \frac{2}{3f} \left( \frac{\alpha q}{k\ell} \right)^2 \right] + \frac{\sqrt{c}}{\sqrt{2}} \frac{1}{D} \left\{ \frac{(D-\varphi_o)^{1/2}}{\varphi_o^{1/2}} \right. \\
& \left. - \frac{(D-\varphi_2)^{1/2}}{\varphi_2^{1/2}} + \frac{1}{D} \left[ \tanh^{-1} \left( 1 - \frac{\varphi_o^{1/2}}{D} \right) - \tanh^{-1} \left( 1 - \frac{\varphi_2^{1/2}}{D} \right) \right] \right\} \quad (95)
\end{aligned}$$

valid for

$$\varphi_1 \leq \varphi_o \leq \varphi_2$$

and

$$\varphi_2 \leq \varphi_m$$

It is seen that the constants  $D$ ,  $G$ ,  $x_s$ ,  $x_p$ , and the distance,  $\rho_1$ , all present themselves as a function of the central cross section curvature  $\varphi_m$ , for a given beam-column. Since  $\varphi_m \geq \varphi_2$ , it is convenient to obtain numerical results by first assuming a value of  $\varphi_m$  and obtaining the corresponding value of  $q$  from Equation (95) by trial and error. Once this is done, the corresponding values of the physical characteristics of the beam-column can be computed in a straightforward manner. Case 3 and Case 6 can be treated in a similar manner.

Case 6 [Fig. 1(c)] - The general solution of the curvature curve of this case is given by Equation (38). The constants  $G$  and  $x_s$  in Equation (38) are given by Equation (91) and Equation (92), respectively. The value of  $\varphi_m$  can be determined from the equation

$$\begin{aligned} \frac{3}{4} k\ell = \left(\frac{\alpha q}{k\ell}\right) \left[ \frac{2}{f} \left(\frac{\alpha q}{k\ell}\right)^2 - \frac{3}{\varphi_m} \right] + \sqrt{f} \left[ \frac{1}{\varphi_o} - \frac{1}{\varphi_m} \right. \\ \left. + \frac{1}{f} \left(\frac{\alpha q}{k\ell}\right)^2 \right]^{1/2} \left[ \frac{1}{\varphi_o} + \frac{2}{\varphi_m} - \frac{2}{f} \left(\frac{\alpha q}{k\ell}\right)^2 \right] \end{aligned} \quad (96)$$

where

$$\varphi_o = \left( \frac{f}{m_{pc} - m_o} \right)^{1/2} \quad (97)$$

valid for

$$\varphi_s \leq \varphi_o$$

and

$$\varphi_s \leq \varphi_m$$

## 15. APPENDIX II - SAMPLE CURVES



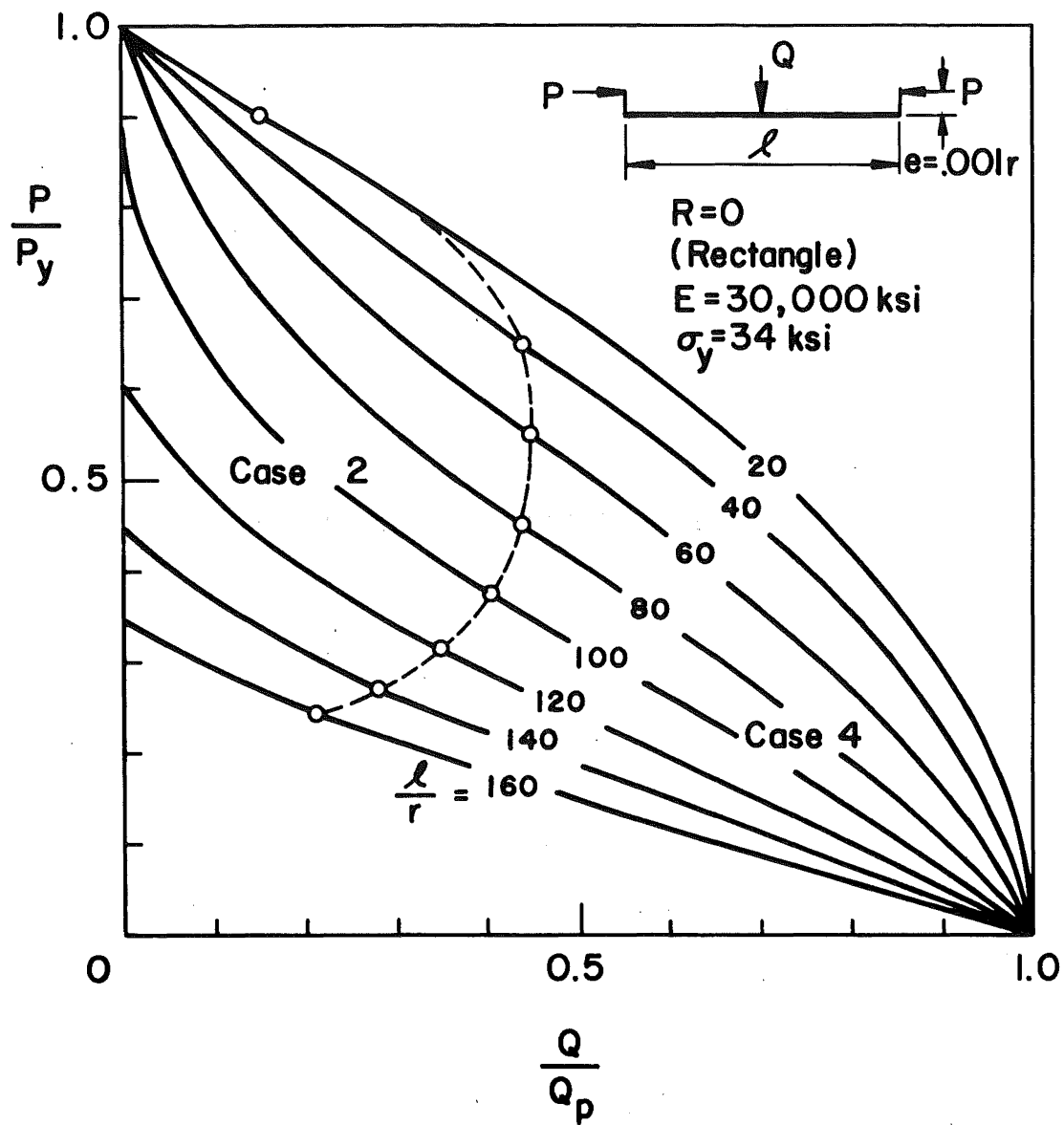


Fig. 18 Interaction Curves for a Rectangular Cross Section with an End Eccentricity

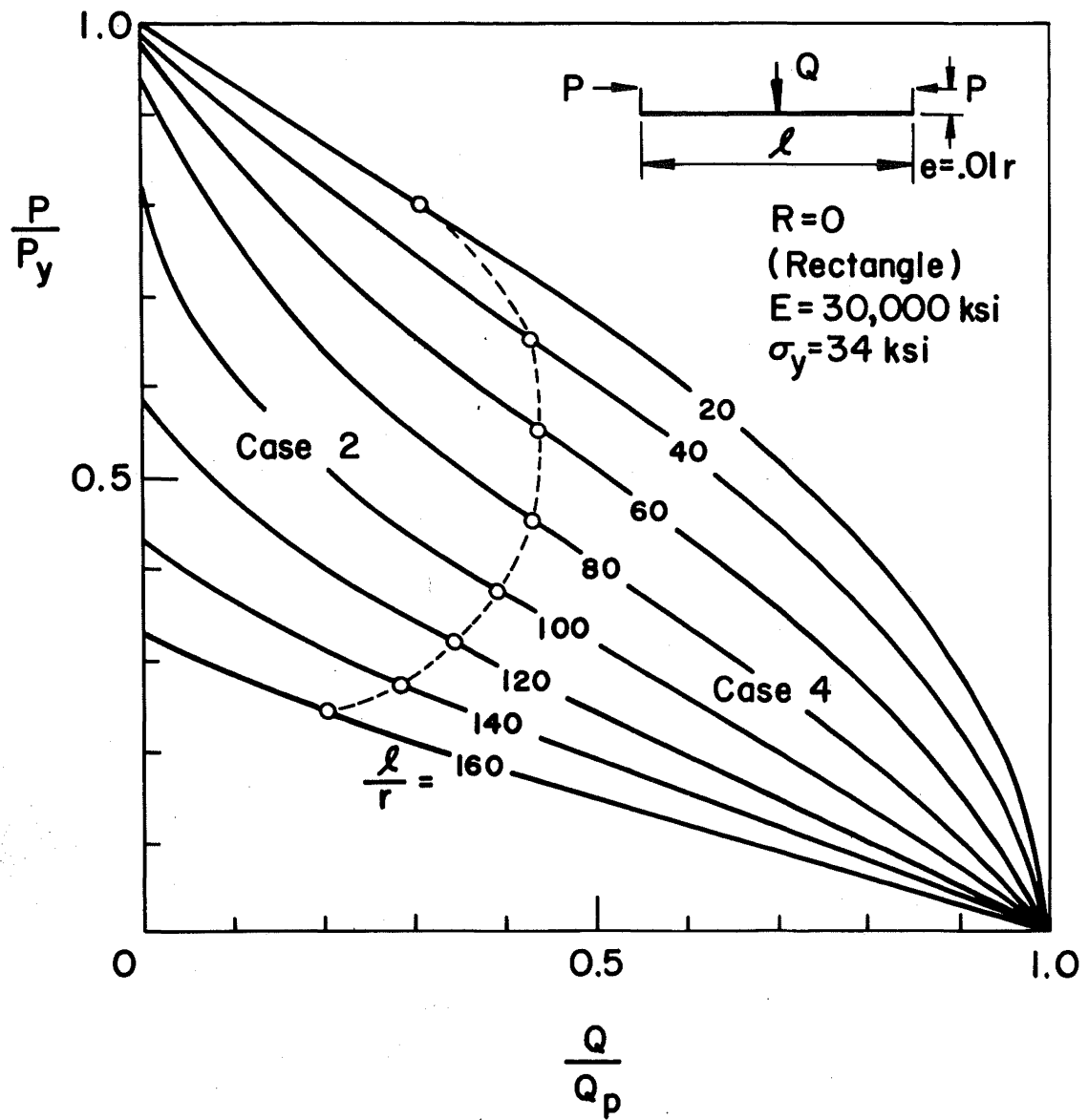


Fig. 19 Interaction Curves for a Rectangular Cross Section with an End Eccentricity

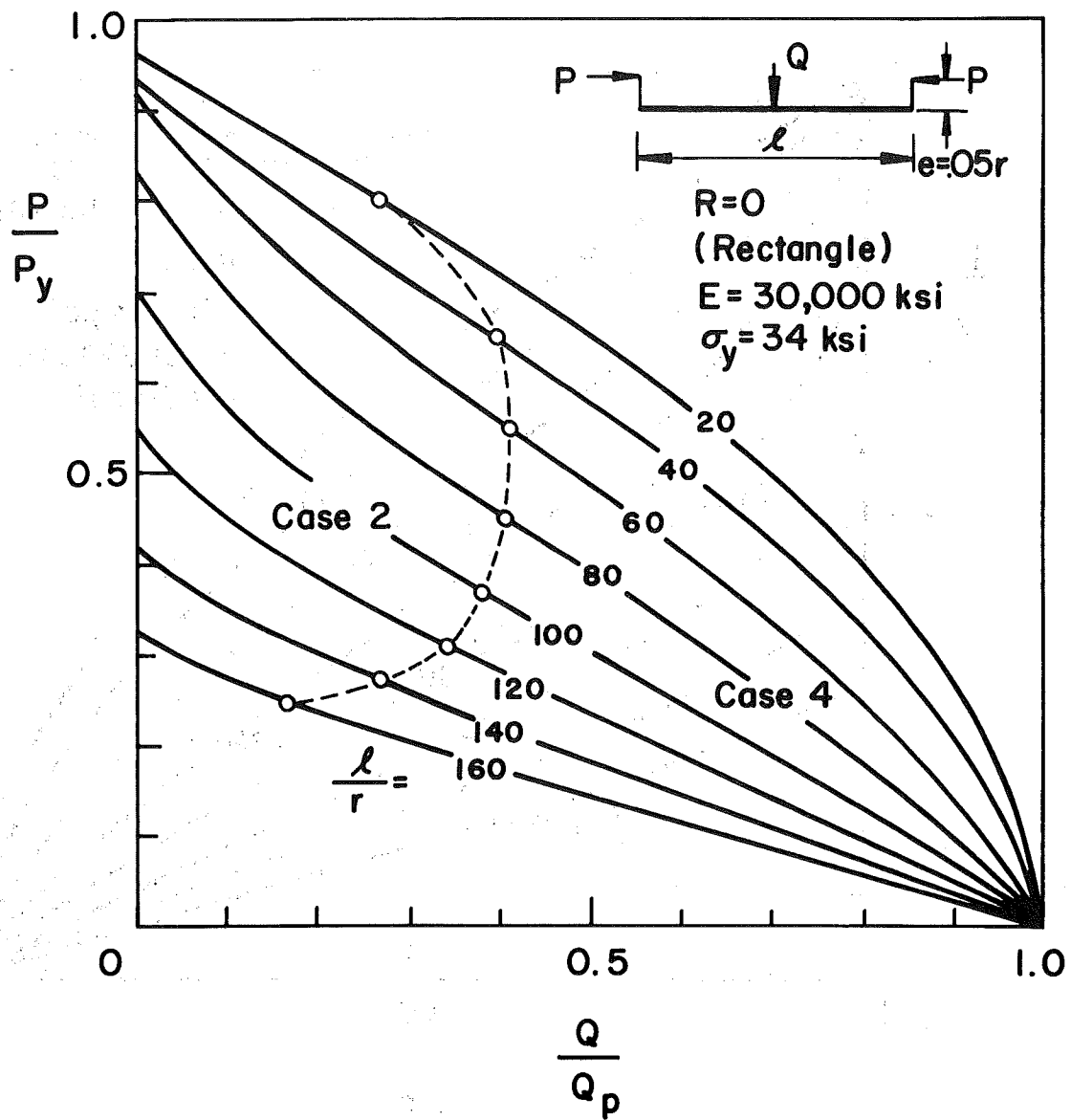


Fig. 20 Interaction Curves for a Rectangular Cross Section with an End Eccentricity

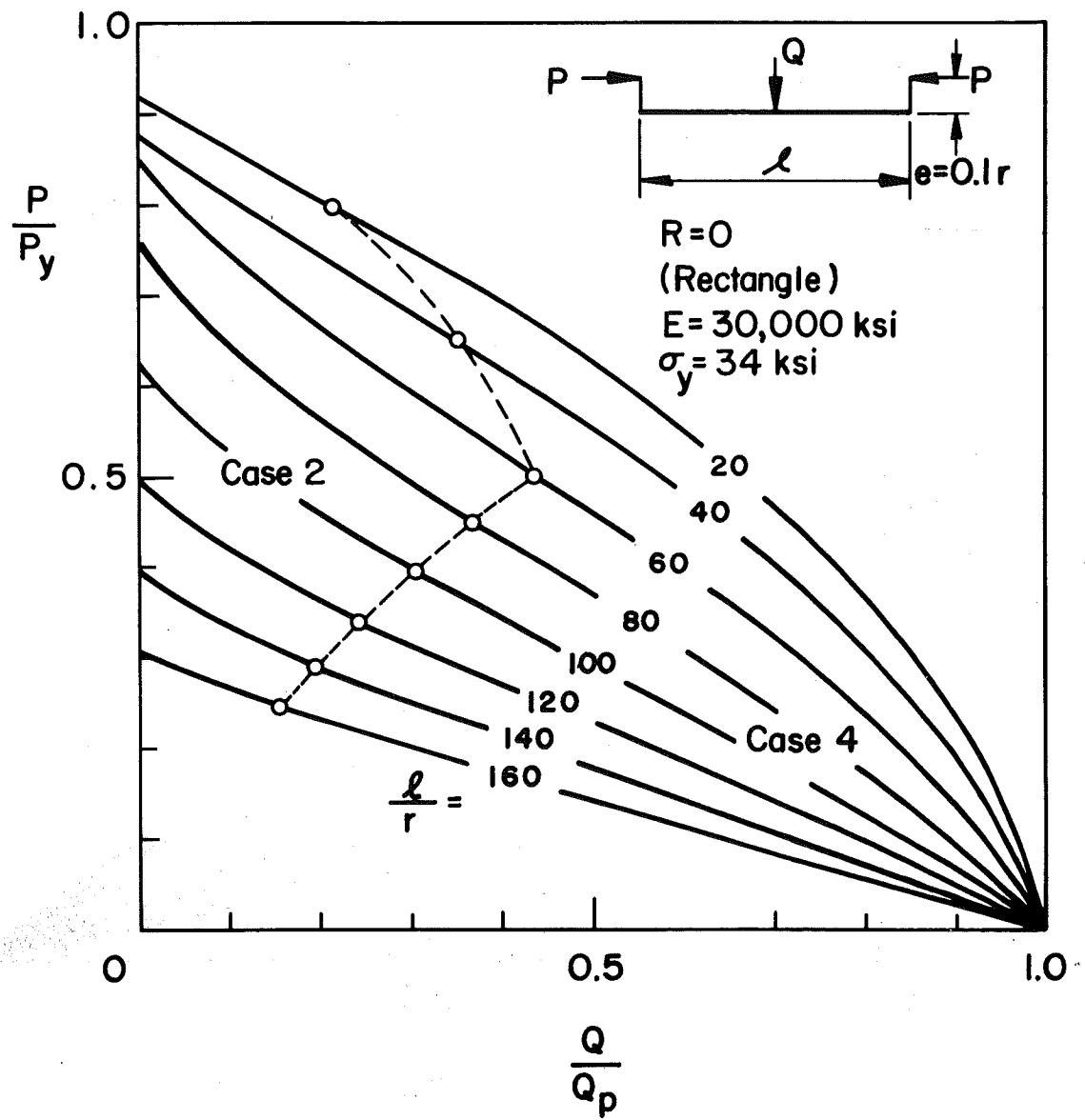


Fig. 21 Interaction Curves for a Rectangular Cross Section with an End Eccentricity

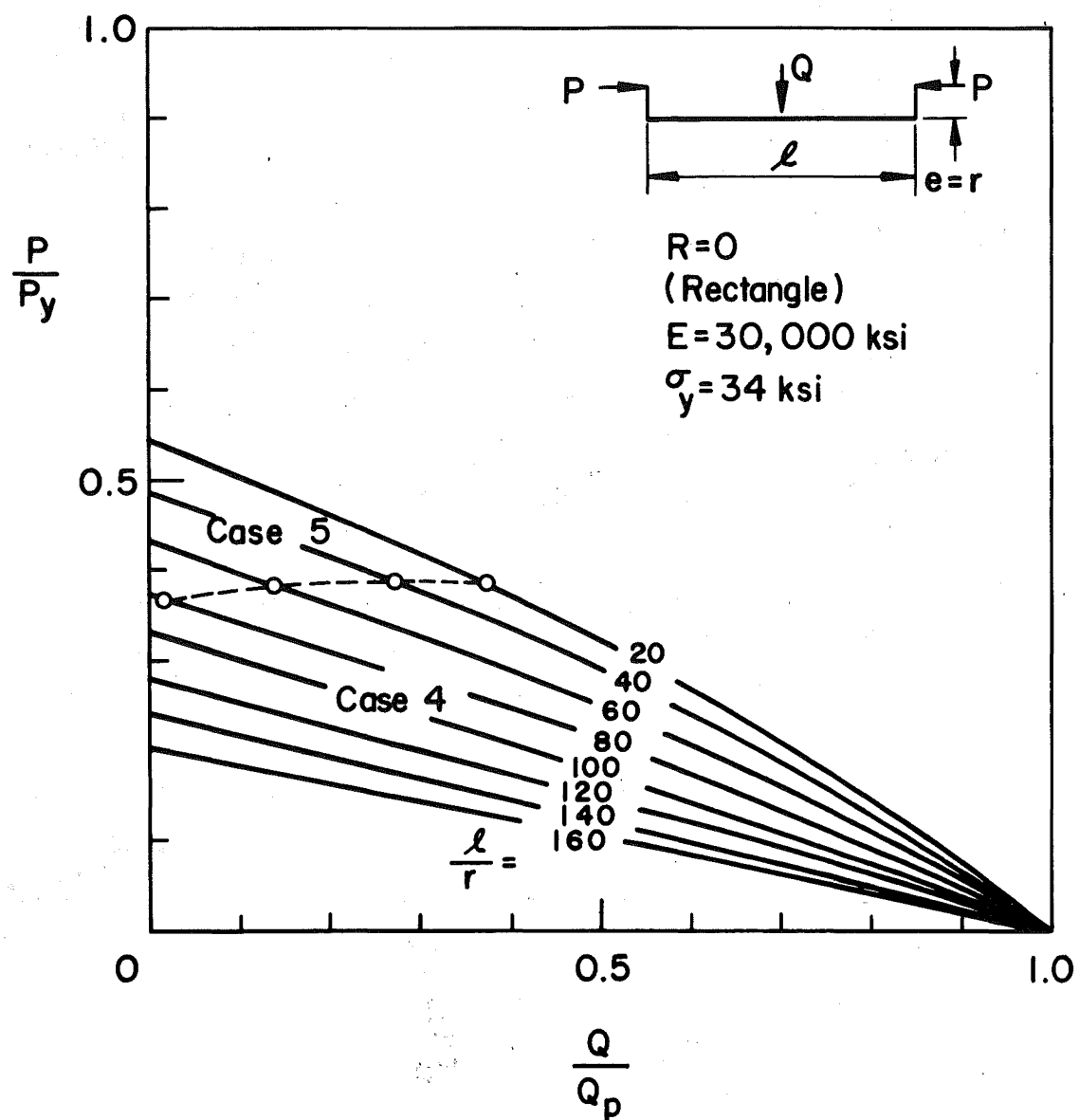


Fig. 22 Interaction Curves for a Rectangular Cross Section with an End Eccentricity

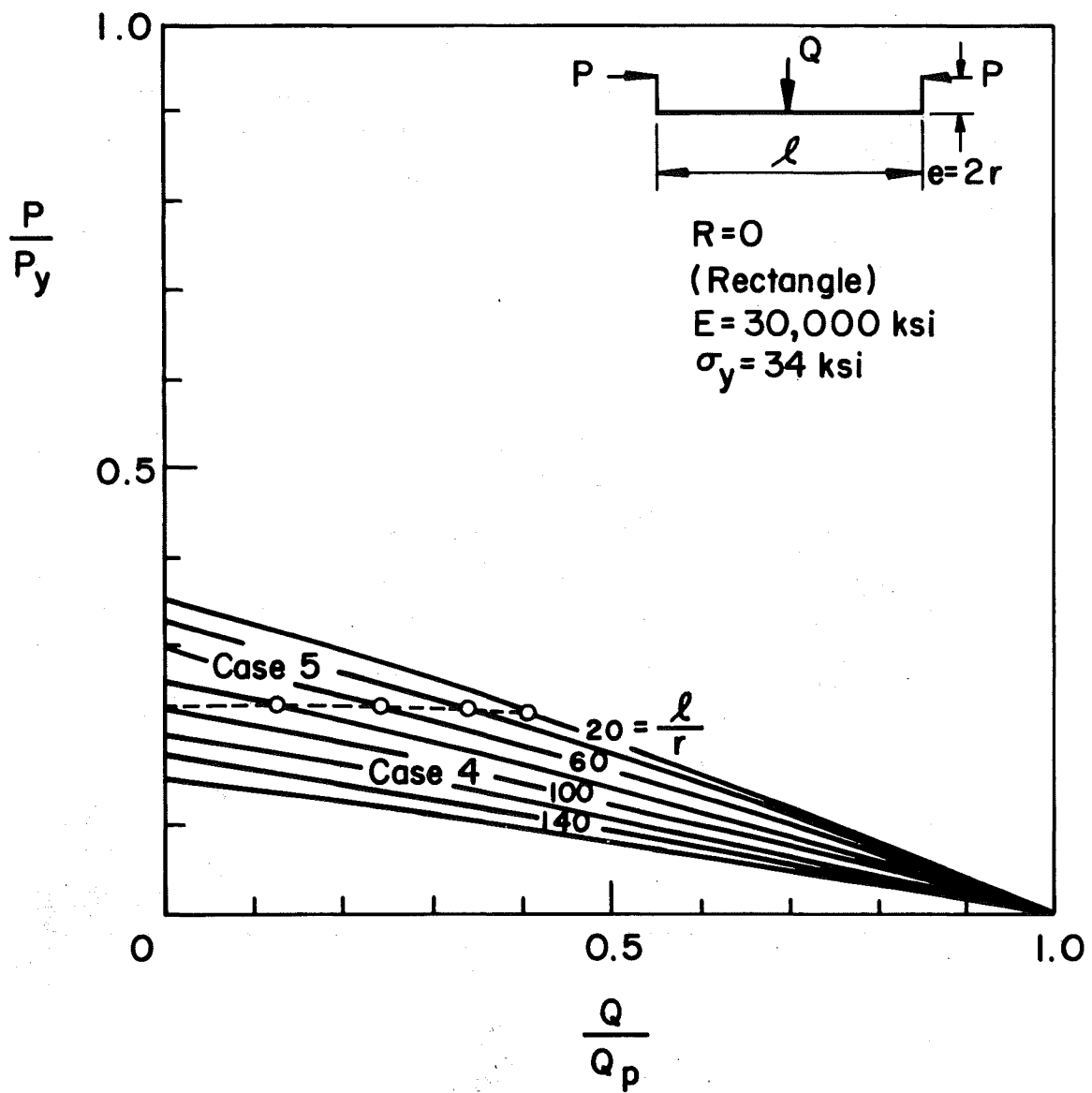


Fig. 23 Interaction Curves for a Rectangular Cross Section with an End Eccentricity

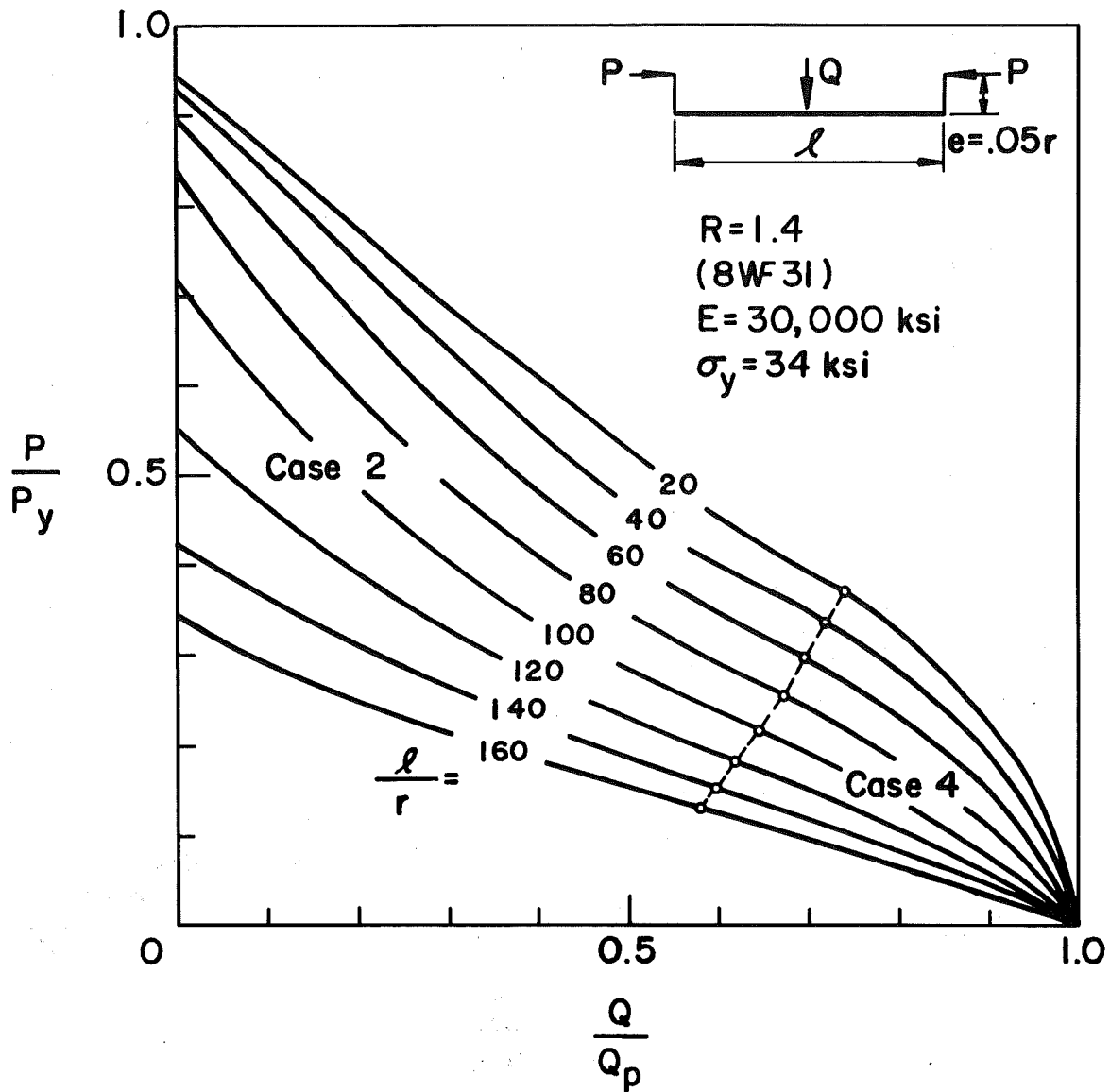


Fig. 24 Interaction Curves for a Wide-Flange Section with an End Eccentricity.

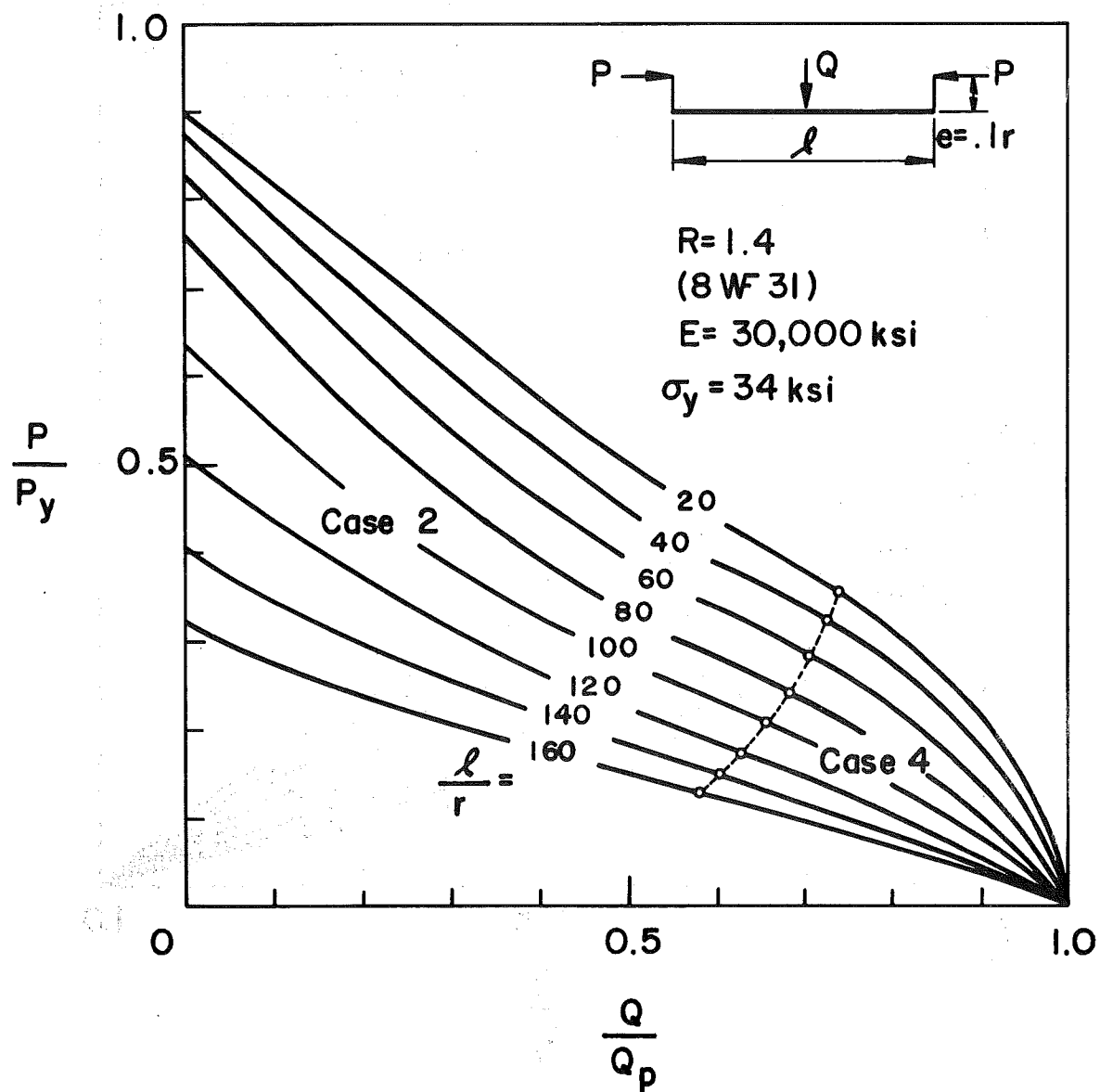


Fig. 25 Interaction Curves for a Wide-Flange Section with an End Eccentricity



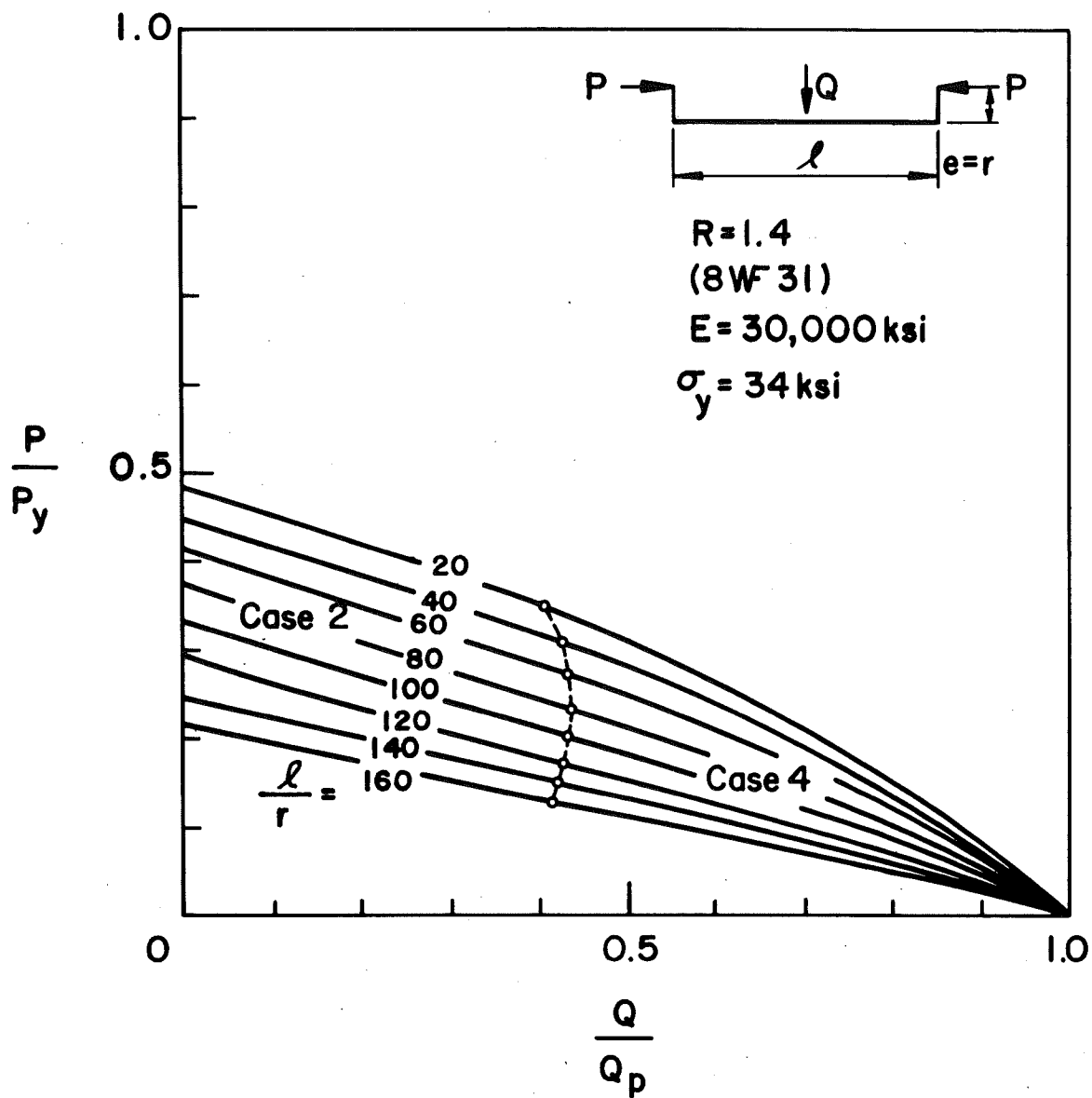


Fig. 26 Interaction Curves for a Wide-Flange Section with an End Eccentricity

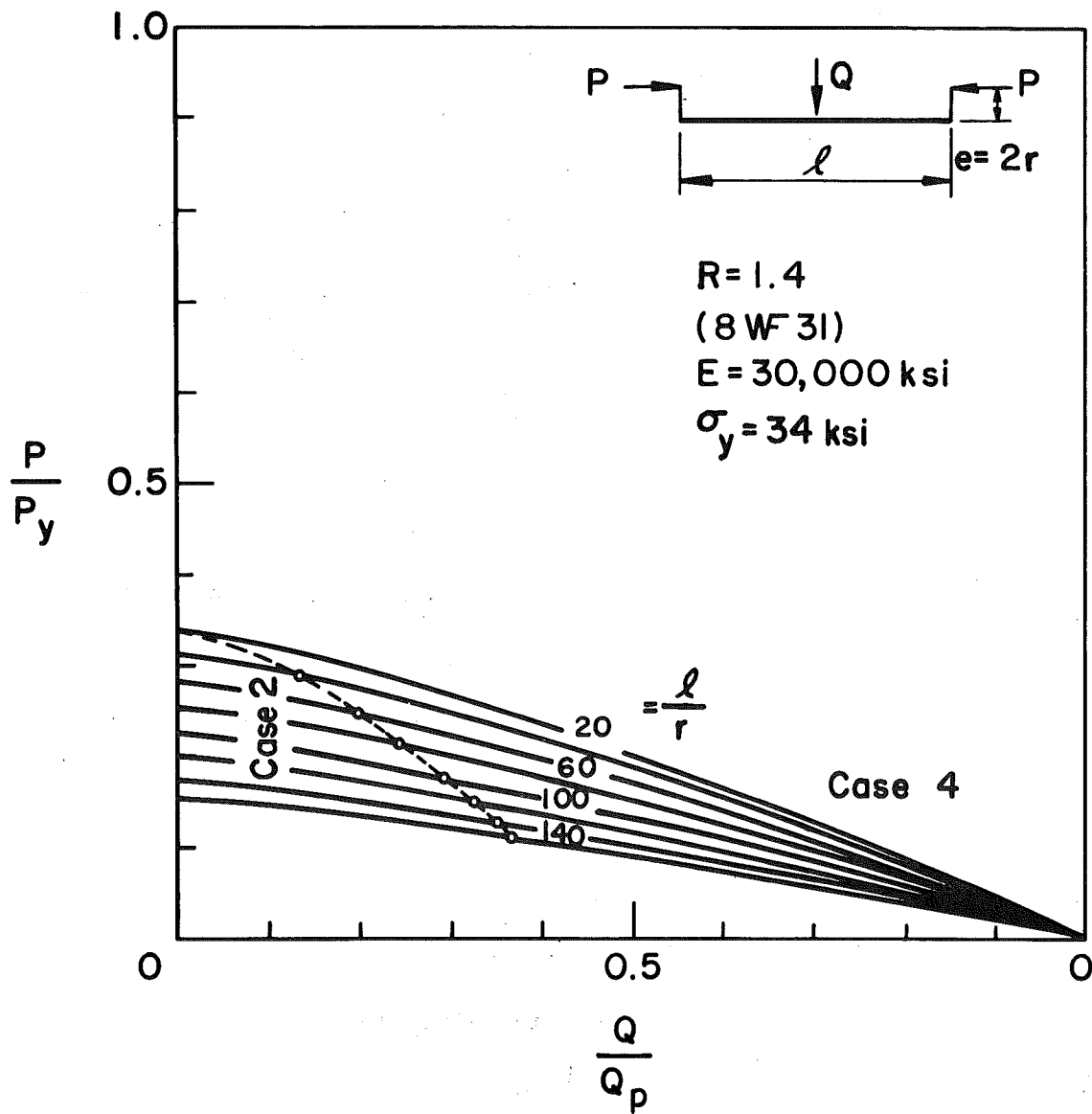


Fig. 27 Interaction Curves for a Wide-Flange Section with an End Eccentricity

## 16. NOTATION

$A$	= area of section
$A_1, B, D, G, x_p, x_s$	= constants of integration
$a, b, c, f, m_1, m_2, m_{pc}, \varphi_1, \varphi_2$	= arbitrary constants define the generalized m- $\varphi$ -p curve
$E$	= modulus of elasticity
$e$	= eccentricity
$h$	= depth of section
$I$	= moment of inertia of section about the axis of bending
$k$	= $\sqrt{P/EI}$
$\ell$	= length of beam-column
$M$	= bending moment
$M_o$	= applied moment at the end of beam-column
$M_y$	= moment which causes first yielding in the section
$m$	= $M/M_y$
$m_o$	= $M_o/M_y$
$P$	= thrust
$P_y$	= axial yield load
$p$	= $P/P_y$
$Q$	= concentrated lateral load
$Q_p$	= plastic limit load according to simple plastic theory

$q$	$= Q/Q_p$
$q_1, q_2, q_3$	$=$ roots of the cubic Equation (72)
$R$	$=$ section variable
$r$	$=$ radius of gyration about the axis of bending
$S$	$=$ elastic section modulus
$x, y$	$=$ coordinate axes
$\alpha$	$=$ shape factor of section about the axis of bending
$\epsilon_y$	$=$ strain at yield point
$\rho_1$	$=$ distance from the end to the primary plastic zone of the beam-column
$\rho_2$	$=$ distance from the end to the secondary plastic zone of the beam-column
$\eta$	$=$ function defined in Equation (60)
$\sigma_y$	$=$ yield stress
$\phi$	$=$ curvature
$\phi_0^*$	$=$ initial curvature
$\phi_m$	$=$ mid-span curvature
$\phi_y$	$=$ curvature at initial yielding for pure bending moment
$\phi$	$= \phi/\phi_y$
$\phi_m$	$= \phi_m/\phi_y$

## 17. REFERENCES

1. Timoshenko, S. P. and Gere, J. M.  
THEORY OF ELASTIC STABILITY, 2nd Edition, McGraw-Hill Book Co., Inc., New York, 1961.
2. Chen, W. F. and Santathadaporn, S.  
CURVATURE AND THE SOLUTION OF ECCENTRICALLY LOADED COLUMNS, Journal of the Engineering Mechanics Division, ASCE, Vol. 95, No. EM1, February 1969.
3. Hauck, G. F. and Lee, S. L.  
STABILITY OF ELASTO-PLASTIC WIDE-FLANGE COLUMNS, Journal of the Structural Division, ASCE, Vol. 89, No. ST6, Proc. Paper 3738, pp. 297-324, December 1963.
4. Wright, D. T.  
THE DESIGN OF COMPRESSED BEAMS, The Engineering Journal, Canada, Vol. 39, p. 127, February 1956.
5. Ketter, R. L.  
FURTHER STUDIES ON THE STRENGTH OF BEAM-COLUMNS, Journal of the Structural Division, ASCE, Vol. 87, No. ST6, Proc. Paper 2910, p. 135, August 1961.
6. Horne, M. R. and Merchant, W.  
THE STABILITY OF FRAMES, Pergamon Press, Inc., New York 1965.
7. Lu, L. W. and Kamalvand, H.  
ULTIMATE STRENGTH OF Laterally Loaded Columns, Journal of the Structural Division, ASCE, Vol. 94, No. ST6, pp. 1505-1523, June 1968.
8. Von Karman, T.  
UNTERSUCHUNGEN UBER KNICKFESTIGKEIT, Mitteilungen Uber Forschungsarbeiten, Herausgegeben Vom Verein Deutscher Ingenieure, No. 81, Berlin, 1910.
9. Chwalla, E.  
AUSSERMITTIG GEDRUCKTE BAUSTAHLSTABE MIT ELASTISCH EINGESPANNTEN ENDEN UND VERSCHIEDEN GROSSEN ANGRIFFSHEBELN, Der Stahlbau, Vol. 15, Nos. 7 and 8, pp. 49 and 57, 1937.
10. Ojalvo, M.  
RESTRAINED COLUMNS, Proc. ASCE, Vol. 86 (EM5), p. 1, 1960.
11. Baker, J. F., Horne, M. R., and Roderick, J. W.  
THE BEHAVIOR OF CONTINUOUS STANCHIONS, Proc. of Royal Society, Serial A, Vol. 198, p. 493, 1949.

12. Ketter, K. L., Kaminsky, E. L., and Beedle, L. S.  
PLASTIC DEFORMATION OF WIDE-FLANGE BEAM-COLUMNS, Trans.  
ASCE, Vol. 120, p. 1028, 1955.
13. Galambos, T. V. and Ketter, R. L.  
FURTHER STUDIES OF COLUMNS UNDER COMBINED BENDING AND  
THRUST, Fritz Laboratory Report No. 205A.19, Lehigh  
University, June 1957.
14. Column Research Council  
GUIDE TO DESIGN CRITERIA FOR METAL COMPRESSION MEMBERS,  
Chapter 6, Edited by B. G. Johnston, John Wiley and  
Sons, Inc., New York, 1966.